

Functional analysis of two photosynthesis related genes (*ASN2* and *PAH2*) in the response to high light

MSc thesis by

René Boesten

920424088090



Supervised by

Roxanne van Rooijen

Mark Aarts

SEPTEMBER 2015

LABORATORY OF GENETICS

WAGENINGEN UNIVERSITY

Table of contents

Abstract	2
Introduction.....	3
High light stress	3
Chlorophyll fluorescence imaging	3
Rationale and previously conducted research	4
Gene functions	6
Aim and objectives	8
Materials and Methods	10
Molecular cloning.....	10
Generation of the triple mutant <i>asn2-1pah1pah2</i>	13
Light experiment	14
Statistics	15
Results	16
Molecular cloning.....	16
Generation of the triple mutant <i>asn2-1pah1pah2</i>	23
Light experiment	24
Discussion	38
Molecular cloning.....	38
Generation of the triple mutant <i>asn2-1pah1pah2</i>	39
Light experiment	40
Acknowledgements	44
References.....	44
Supplemental data	47

Abstract

Light is the driving force that provides, by definition, the energy for the most important biological process: photosynthesis. However, when more photons are absorbed by the chloroplasts than can be used to drive photosynthesis, light can induce stress in plants which is known as high light stress. In this research two photosynthesis related genes, *ASPARAGINE SYNTHETASE 2 (ASN2)* and *PHOSPHATIDIC ACID PHOSPHOHYDROLASE 2 (PAH2)*, are studied in *Arabidopsis thaliana*. *ASN2* encodes a nitrogen transport compound that affects the plants nitrogen status while *PAH2* is involved in substrate provision for galactolipid synthesis. These two genes were found to be in epistasis, however it still has to be proven that natural genetic variation in these genes is causing the variation in photosynthesis. The two alleles from these genes that are considered to cause a high photosynthesis efficiency response are cloned. These constructs can be used in an allelic complementation test to validate that the natural variation in these genes is causing the photosynthesis phenotype to high light. Furthermore, the hypothesis that both of these genes exert their photosynthetic response to high light via alterations in the chloroplasts membranes through galactolipid synthesis is tested. This hypothesis was tested in an experiment in which wild type, two extreme natural accessions Ts-1 (low photosynthesis efficiency) and Ga-0 (high photosynthesis efficiency) and the T-DNA insertion knock out mutants *asn2-1*, *pah1pah2* (*PAH1* functions redundantly with *PAH2*) and the newly obtained *asn2-1pah1pah2* were grown under low light intensity and subsequently moved to high light intensity. Chlorophyll fluorescence imaging in combination with quantitative real-time PCR of all *Arabidopsis* mono- and digalactosyldiacylglycerol synthase genes (*MGD1*, *MGD2*, *MGD3*, *DGD1* and *DGD2*) that produce the main constituents of chloroplast membranes support this hypothesis. Furthermore, expression analysis and chlorophyll fluorescence imaging data in the mutant lines have provided more evidence of the epistatic interaction between *ASN2* and *PAH2*.

Introduction

High light stress

Light is of extreme importance to plants, as it is used for photosynthesis but also for regulating development. Plants are equipped with a set of photoreceptors which enables plants to sense the direction, wavelength, intensity and duration of the light (**Kagawa et al. 2001**). These cues are used, amongst others, to optimise photosynthesis, for instance by adjusting direction of growth towards light (phototropism), leaf angle adjustments and relocation of chloroplasts in the leaves.

High light exposure can cause light stress to plants. This can occur when more light is absorbed by the chloroplasts than can be used to drive photosynthesis. Plants experience fluctuations in light exposure on a daily basis, such as under full sun light in the middle of the day, but also on a seasonal basis, when comparing summer and winter sun light. Aside from high light conditions, stress can also occur when the plant's photosynthetic capacity is low, for example by water or chilling stress (**Demmig-Adams and Adams 1992**). When an excess of light energy is converted into chemical energy, this energy has the potential to be transferred to oxygen. This results in the formation of reactive oxygen species (ROS) such as hydrogen peroxide (H_2O_2), singlet oxygen ($^1\text{O}_2$), superoxide (O_2^-) and the hydroxyl radical (OH^\cdot) (**Karpinski et al. 1997**). ROS can oxidise (crucial) enzymes, lipids and proteins which can cause damage to the photosynthetic apparatus or other parts of the cell. This could lead to restricted growth or leaf death, pigment bleaching and, in extreme cases, death of the plant (**Demmig-Adams and Adams 2006**) (**Müller et al. 2001**).

Under conditions without major restrictions to growth, plants are well equipped to cope with an excess of light energy. The photosynthetic apparatus is capable of responding to the environment (photosynthetic acclimation). Different strategies can be used to reduce oxidative stress by excess light, which can be short or long term strategies based on avoiding or coping with stress. Strategies include dissipation of excess light energy as heat, and changes in both leaf thickness and the number and position of chloroplasts. Furthermore, changes in structure and function of the photosynthetic apparatus are found such as changes in the activation state of Rubisco, regulation of photosystem II (PSII) efficiency (**Bailey et al. 2001**) and the size of the light harvesting pigment antennae (**Müller et al. 2001**).

Chlorophyll fluorescence imaging

The efficiency in which light is used by the photosynthetic apparatus can be measured by chlorophyll fluorescence imaging. There are three fates that light energy that is absorbed by chlorophyll can undergo. Most importantly, light energy can drive photosynthesis. Excess light energy that is not used to drive photosynthesis can be dissipated as heat or be emitted as light. These three fates occur in competition (**Maxwell and Johnson 2000**). When a plant is transferred from darkness into light, PSII reaction centers are closed which increases the fluorescence level during the first second (**Maxwell and Johnson 2000**). After this, the yield of chlorophyll fluorescence drops during a few minutes. This is known as fluorescence quenching and can be explained in two ways: via photochemical and non-photochemical quenching. Photochemical quenching is known as the opening of stomata and the light-induced activation of enzymes involved in carbon metabolism that cause an increase in the rate of electron transport away from PSII. Non-photochemical quenching on the other hand is known as the increase in efficiency in which energy is converted into heat (**Maxwell and Johnson 2000**). Plants first have to be dark adapted in order to reach a steady state between

photochemical and non-photochemical quenching. A useful parameter that can be measured is the quantum yield of PSII (Φ_{PSII}) photochemistry, which is a measurement of the proportion of light that is absorbed by chlorophyll associated with PSII which is used during photosynthesis (Maxwell and Johnson 2000). Φ_{PSII} provides insight in PSII functioning, as it gives insight in how excess light is absorbed and is indirectly damaging PSII when the light energy is converted into ROS. It also provides a measure of the rate of linear electron transport and is thereby indicative of the overall rate of photosynthesis (Maxwell and Johnson 2000).

Rationale and previously conducted research

High light stress is a common kind of stress affecting many plants, including crops. Getting better insights into the pathways and genetic regulation of photosynthesis under high light is therefore important from a fundamental perspective, while this information has also potential to improve crops. Natural genetic variation is a tool that can be applied to find these underlying genetic mechanisms (Flood et al, 2011). In previous experiments, the response to high light stress was measured among *Arabidopsis thaliana* natural accessions (Van Rooijen et al, 2015). Plants were initially grown at low light intensity ($100 \mu\text{mol photons m}^{-2} \text{s}^{-1}$) and subsequently after two weeks exposed to high light intensity ($550 \mu\text{mol photons m}^{-2} \text{s}^{-1}$). During the experiment the photosynthetic light use efficiency (Φ_{PSII}) was measured to monitor the photosynthetic response. The experiment showed natural variation for the photosynthesis efficiency response to high light. Genome wide association studies (GWAS) and F2 family mapping studies have unveiled an epistatic interaction between two genes; *ASPARAGINE SYNTHETASE 2* (*ASN2*) and *PHOSPHATIDIC ACID PHOSPHATASE 2* (*PAH2*). Only when for both of these genes a 'low' photosynthetic efficiency allele is present, the photosynthesis efficiency upon high light intensity is low and significantly different from other allelic combinations (Figure 1).

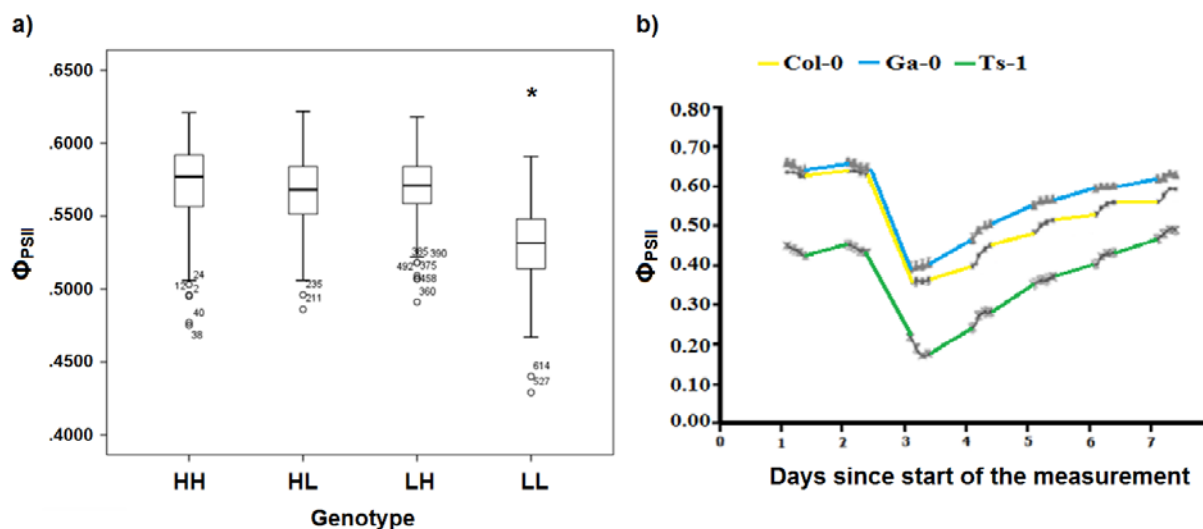


Figure 1: Epistatic interaction between *ASN2* and *PAH2*. a) Boxplot of the photosynthesis efficiency (Φ_{PSII}) of groups of accessions with different combinations of alleles for *ASN2* and *PAH2* (HH: high allele *ASN2*, high allele *PAH2* – HL: high allele *ASN2*, low allele *PAH2* – LH: low allele *ASN2*, high allele *PAH2* – LL: low allele *ASN2*, low allele *PAH2*). Only when for both genes a low allele is present (LL), a significant lower Φ_{PSII} is obtained (denoted with *). b) Φ_{PSII} response over time for reference accession Col-0 (yellow) and accessions with contrasting combinations of alleles (Ga-0 has both high alleles (blue); Ts-1 has both low alleles (green)). Plants were grown at $100 \mu\text{mol photons m}^{-2} \text{s}^{-1}$ for the first two days of the experiment and subsequently exposed to $550 \mu\text{mol photons m}^{-2} \text{s}^{-1}$ for the remaining days

Based on sequence information from the *Arabidopsis* 1001 genome browser (<http://signal.salk.edu/atg1001/3.0/gebrowser.php>), different alleles have previously been selected for these two genes. This was done by comparing the sequence of many resequenced accessions with Col-0 (reference accession) (Van Rooijen et al, unpublished). Polymorphisms within these genes are present in the HapMap population (Figure 2) (Weigel and Mott, 2009). The polymorphisms that were previously selected, were either significantly correlated in a genome wide association study, or were in LD with SNPs that were significantly correlated. Furthermore, the selected polymorphisms segregated in opposite ways with the extreme photosynthesis phenotype in the *Arabidopsis* 1001 genome browser (Van Rooijen et al, unpublished). The different previously selected polymorphisms and alleles are listed in Table 1. Each allele is characterised by a specific combination of two SNPs. The alleles that consists of two non-Col-0 SNPs are not present in the HapMap population, and therefore three alleles per gene are found within the population: an intermediate Col-0 allele, a 'high' photosynthesis efficiency allele (found in the Ga-0 accession) and a 'low' photosynthesis efficiency allele (found in the Ts-1 accession) (Figure 2).

Table 1: Selected polymorphisms in *ASN2* and *PAH2*.

Gene	Position on <i>Arabidopsis</i> 1001 genome browser	Nucleotide	Amino acid	Allele	Photosynthesis efficiency phenotype
<i>ASN2</i>	25.970.333	A	-	Col-0	Low
		G	-	Non Col-0	High
	25.971.571	A	Glutamine	Col-0	High
		C	Aspartic acid	Non Col-0	Low
<i>PAH2</i>	17.187.895	A	-	Col-0	High
		G	-	Non Col-0	Low
	17.188.123	T	Asparagine	Col-0	Low
		A	Isoleucine	Non Col-0	High

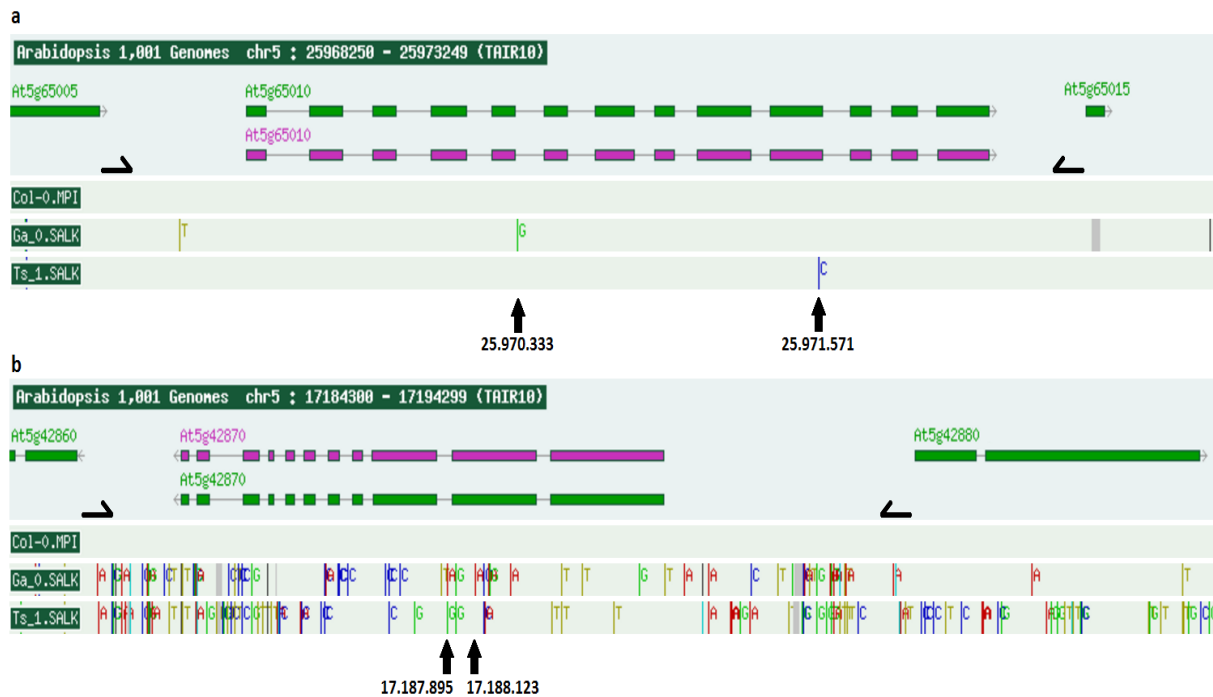


Figure 2: Selected polymorphisms for *ASN2* (a) and *PAH2* (b). For both genes three alleles are designated that segregate with a photosynthesis phenotype. In the top lane the structure of the gene is given with green and purple boxes that represent exons. The sequence of Col-0, in the lane below, is used as a reference sequence. Sequence differences in the accessions Ga-0 and Ts-1 compared to Col-0 are depicted as coloured stripes with a nucleotide code adjacent to it. The Ga-0 accession has for both genes a ‘high’ allele while Ts-1 has both ‘low’ alleles. The black arrows show the selected polymorphisms with the position information from the *Arabidopsis* 1001 genome browser. Black half arrows show the positions of primers that were used in the cloning approach; directly bordering the adjacent genes.

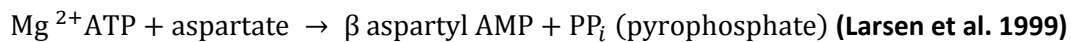
Gene functions

ASPARAGINE SYNTHETASE 2 (ASN2) is one of three members of the small asparagine synthetase gene family in *Arabidopsis* (Gaufichon et al. 2013). Asparagine (Asn) acts as a nitrogen transport compound which can store and/or transport nitrogen from sources to sinks (Lam et al. 1998). Asparagine synthesis is strongly regulated by light and metabolites in many plants, including *Arabidopsis* (Lam et al. 1998). Asn levels are high in the dark and are repressed by light treatment. *ASN1* expression, but not *ASN2*, correlates with the high Asn levels in the dark. In fact, an opposite expression pattern is found for *ASN2* whereby *ASN2* expression is induced by light in dark-adapted plants; this induction of expression is ammonium dependent (Lam et al. 1998) (Wong et al. 2004). Ammonium is an important intermediate in nitrogen assimilation. Endogenous free ammonium accumulation occurs upon different kinds of stress, including water, cold, salinity and high light stress (Wong et al. 2004). Free Asn levels are induced upon these different kinds of stress and can account for up to 7% of total nitrogen under high light stress (Huber et al. 1984) (Sieciechowicz et al. 1988). Asn is proposed to play a role in ammonium metabolism, whereby ammonium is used for asparagine assimilation (Wong et al. 2004). *ASN2* overexpressing lines accumulated significantly less ammonium compared to wild type and underexpressing lines when the concentration of ammonium was increased from 20 to 50 mM ammonium (Wong et al. 2004). Furthermore, under high light irradiance *ASN2* underexpressors showed significantly higher levels of ammonium (Wong et al.

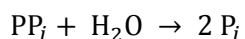
2004). A similar response was seen by **(Gaufichon et al. 2013)** whereby *asn2-1* knockout lines showed an increase of 20% in ammonium concentration.

Ammonium levels increase under high light irradiance which induces expression of *ASN2*, and thereby increases Asn levels. This affects the nitrogen status of the plant. Nitrogen is a key nutrient for photosynthesis, since the vast majority of leaf nitrogen content is incorporated in proteins from the Calvin cycle and thylakoid membrane **(Evans 1989)**. In *asn2-1* and *asn2-2* (knockout mutant and underexpressor with 80% reduction in *ASN2* expression compared to Col-0 respectively) the rosette leaves contained 11 to 12% less total nitrogen, while also the chlorophyll content was decreased by 40% and 20% respectively compared to wild type **(Gaufichon et al. 2013)**

The *ASN2* protein has two distinct active sites; an N-terminal hydrolysis domain for the hydrolysis of glutamine, and a C-terminal synthetase domain. In the 'low' allele, a SNP is present in the C-terminal synthetase domain which leads to an amino acid change from glutamine (E) to aspartic acid (D). The C-terminal synthetase domain is an ATP-pyrophosphatase (ATP-PPase) domain responsible for the following reactions:



PP_i is unstable in aqueous environments and hydrolyses into P_i in the reaction:

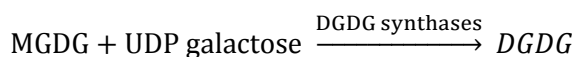
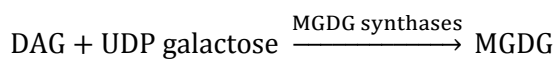
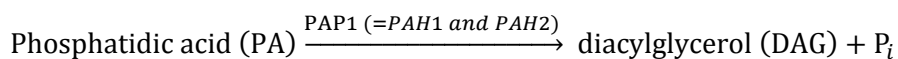


The other gene thought to explain part of the natural variation for photosynthesis acclimation to high light stress is *PHOSPHATIDIC ACID PHOSPHOHYDROLASE 2 (PAH2)* which functions redundantly with *PAH1* **(Eastmond et al. 2010a)**. Both *PAH1* and *PAH2* are active under phosphate-limiting conditions in membrane lipid remodelling where they are involved in converting phospholipids into galactolipids **(Nakamura et al. 2009)**. For example, in the *pah1pah2* double mutant the galactolipids mono- and di-galactosyldiacylglycerol (MGDG and DGDG) decreased by 16% and 30% respectively, while the phospholipids phosphatidylcholine (PC) and phosphatidylethanolamine (PE) increased by 47% and 20% respectively compared to Col-0 **(Nakamura et al. 2009)**. Biogenesis of plastid membranes is essential for photoautotrophic growth, which requires a significant increase in galactolipids **(Kobayashi et al. 2007)**. These galactolipids provide the matrix in which the photosynthetic apparatus is embedded. MGDG and DGDG are some of the main constituents of chloroplast membrane lipids and compose 52 and 26 weight percent of fatty acids in spinach thylakoids respectively **(Block et al. 1983)**. Except for providing the matrix for the photosynthesis apparatus, galactolipids also play a more direct role in photosynthesis. MGDG and DGDG, amongst other galactolipids, have been found tightly bound to the reaction centres of photosystem I (PSI) and PSII in x-ray crystallographic analysis **(Kobayashi et al. 2007)**. The ratio of MGDG over DGDG is important for membrane stability, and is involved in intracellular protein trafficking and protein folding in the chloroplast **(Chen et al. 2006)**. Furthermore, this ratio plays a crucial role in thermotolerance **(Chen et al. 2006)**.

MGDG is produced from UDP-Galactose (UDP-Gal) and diacylglycerol (DAG) by MGDG synthases (MGD) at the plastid envelopes. Subsequently, another UDP-Gal can be added by DGDG synthases (DGD) to form DGDG **(Nakamura et al. 2009) (Li et al. 2012)**. Two pathways of DAG provision for

galactolipid synthesis exist in *Arabidopsis*: the prokaryotic pathway which is located at the plastids, and the eukaryotic pathway located at the endoplasmic reticulum (ER) (**Eastmond et al. 2010b**). Both pathways rely on phosphatidic acid phosphatase (PAP) activity that dephosphorylates phosphatidic acid (PA), a precursor for all phospholipids, to obtain both the substrate DAG and inorganic phosphate (P_i) (**Nakamura and Ohta 2010, Eastmond et al. 2010b**). Two classes of PAP exist that can be distinguished based on their enzymatic properties. PAP1 are magnesium (Mg^{2+}) dependent PAPs that are soluble enzymes which localize both at the ER and chloroplasts (*PAH1* and *PAH2* encode PAPs of this class) (**Nakamura and Ohta 2010**). PAP1 is proposed to play a role in the Kennedy pathway (in the Kennedy pathway first PA is synthesized which is then dephosphorylated by PAP to produce DAG) and its protein was identified as the first PAP in the yeast *Saccharomyces cerevisiae* (**Han et al. 2006**). *PAH2* was found to be identical to the yeast homolog of Lipin, a known key regulator in lipid metabolism, and was named phosphatidate phosphohydrolase (PAH) (**Nakamura and Ohta 2010**). The other class of PAPs, PAP2, is considered to mainly function in signalling. PAP2 are independent of Mg^{2+} and dephosphorylates other lipid phosphatases other than PA (**Nakamura and Ohta 2010**).

Important reactions in membrane remodelling:



In summary, *PAH1* and *PAH2* are both PAPs that are active under phosphate limiting conditions (**Nakamura and Ohta 2010**). The substrate DAG for the non-phosphorous galactolipids MGDG and DGDG is formed by dephosphorylation of PA, leaving P_i as side product. *MGD1* and *DGD1* are the most important genes from the MGDG and DGDG synthases and produce the bulk of galactolipids in chloroplasts (**Benning and Ohta 2005**). Mutants for either of these two genes are severely impaired in photosynthesis (**Benning and Ohta 2005**). Under phosphate limiting conditions high amounts of DGDG are accumulated, which also occurs through increased *DGD2* (which encodes for a DGDG synthase) expression (**Kelly and Dörmann 2002**). On the other hand, under nitrogen limiting conditions both *DGD1* and *DGD2* are also up-regulated, independent from the phosphate status of the plant (**Gaude et al. 2007**). *ASN2* is known to be affected by light in combination with increased ammonium, which can be induced by high light irradiance, and can thereby affect the nitrogen status and thus indirectly affect the lipid composition via the MGDG and DGDG synthases. Furthermore, *ASN2* generates two inorganic phosphates ($2 P_i$). Therefore, my hypotheses are, that *ASN2*, *PAH1* and *PAH2* are involved in releasing P_i , which is an important nutrient for the photosynthesis apparatus. Furthermore, these three genes might directly or indirectly (*ASN2*) affect expression of the MGD and DGD synthases. This could result in differences in chloroplast membrane stability and thereby affect photosynthesis.

Aim and objectives

The aim of this study is to understand the roles of *ASN2* and *PAH2* in the photosynthetic response to high light. The first objective is to determine if genetic variation in *ASN2* and *PAH2* is causing the differential response in photosynthesis to high light. The second objective of this research is to

obtain the *asn2-1pah1pah2* triple mutant. My hypothesis is that this triple mutant will have relatively low photosynthesis efficiency compared to Col-0, *asn2* and *pah1pah2*. The triple mutant can be complemented by both 'high' alleles in a transgenic approach. If this double transformant has higher photosynthesis efficiency compared to Col-0, this could serve as a final proof of the epistatic interaction of these two loci. The third objective is to measure expression of *ASN2*, *PAH1* and *PAH2* in Col-0 (reference accession), *asn2-1*, *pah1pah2*, *asn2-1pah1pah2* and two natural accessions that harbor either both 'low' or 'high' alleles (Ts-1 and Ga-0 respectively). This will provide more insights into the interaction between *ASN2* and *PAH2*. The fourth objective of this project is to test the hypothesis that both *ASN2* and *PAH2* exert their photosynthetic effect via lipid remodeling of photosynthetic membranes. Overall, this research can provide more insight in photosynthesis related processes in plants, and how plants cope with light stress. Specifically, this research might give better insight in the response of *Arabidopsis* to high light stress and can test if the allelic variation in the candidate genes is indeed causing a part of the natural variation in photosynthesis efficiency.

For the first objective, both 'high' and 'low' alleles from both genes will be cloned in order to perform an allelic complementation test. Previous results have shown that both 'high' alleles are dominant over the 'low' alleles (**Van Rooijen et al. unpublished**). Therefore, in this complementation test both 'high' alleles will be introduced separately into multiple accessions that harbor both 'low' alleles. The hypothesis is that photosynthesis efficiency will increase in all of these transformants. The constructs will contain the endogenous promoter, coding region and terminator. Hereby plants are created which now contain a 'high' allele from one of the genes, and a 'low' allele from the other gene. The mode of action of the different alleles is currently unknown, therefore expression differences might be causing the photosynthetic phenotype. Multiple copies of the transgene might be incorporated into the genome during the transformation, and therefore a dosage effect could occur. This could mean that the introduced 'high' allele is expressed to a higher extent that is independent from expression differences due to the allelic variation. As a control, constructs will be made from the 'low' alleles and will be used to transform the same accessions as the accessions that are transformed with the 'high' alleles. In this control, the photosynthesis efficiency is expected to be unaffected compared to the (same) untransformed accession. This control is incorporated to make sure that only the effect of the allelic variation is seen, and not the effect of the transformation procedure or a dosage effect.

For the second objective, a number of offspring from previously made crosses between *pah1pah2* and *asn2-1* will be genotyped by PCR. To test the third and fourth hypothesis, different genotypes will be subjected to 1) continuous low light intensity; 2) continuous high light intensity and 3) low light intensity and subsequently moved to high light intensity and two intermediate light intensities (4 and 5). Expression of all *Arabidopsis* MGD and DGD synthases will be measured by qRT-PCR from plants under continuous low light and plants that received high light for 3 hours. Also extra plants will be grown for lipid analysis, although this analysis will not be performed in this project.

Materials and Methods

Molecular cloning

Gateway cloning

Two electro-competent strains of *Escherichia coli* were prepared; TOP10 (susceptible to the *ccdB* cassette) for multiplication of entry and expression vectors (*Supplemental data, Protocols, Preparation of electro competent cells*), and DB3.1 (resistant to the *ccdB* gene) for multiplication of donor and destination vectors (*Supplemental data, Protocols, Preparation of electro competent DB3.1 E. coli cells*). Transformation efficiency of these cells was determined by transforming both strains with *pUC19* via electroporation (*Supplemental data, Protocols, Transformation by electroporation*) and subsequently plating on LB+50 µg/µL ampicillin.

pDONR201 (<https://www.thermofisher.com>), *pDONR221* (<https://www.thermofisher.com>), *pBGW* (<https://gateway.psb.ugent.be/>) (**Figure 3**) and *pKGW_RedSeed* (<https://gateway.psb.ugent.be/search>) (**Figure 3**) were introduced into *E. coli* DB3.1 via electroporation and subsequently grown overnight at 37°C on selective medium (*pDONR201/pDONR221* on 50 µg/µL kanamycin; *pBGW/pKGW_RedSeed* on 50 µg/µL spectinomycin). Single colonies were picked with a sterile toothpick and grown overnight in 5 mL LB medium with antibiotic (same type and concentration of antibiotics as LB plates). The same colonies were also inoculated on new selection plates for possible further use. Vectors were isolated using a Qiagen miniprep kit and analysed on a 1% agarose gel by restriction enzyme digestion. Colonies containing correct vectors were grown overnight in 2 mL selective medium. Glycerol stocks (25% glycerol) were made from these cultures by adding 500 µL 50% glycerol to 500 µL of the overnight culture. Glycerol stocks were frozen in liquid nitrogen and stored at -80°C.

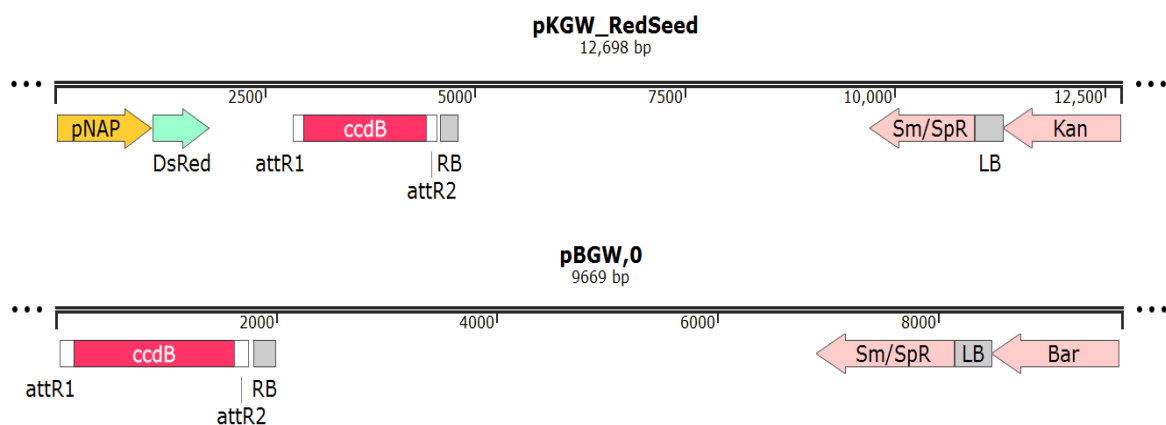


Figure 3: Schematic vector map of *pKGW_Redseed* (top) and *pBGW* (bottom). Double black lines represent DNA sequences, with the nucleotide position indicated below. Coloured arrows are different features on the vector: antibiotic resistance (pink arrows: Sm/SpR: spectinomycin; Kan: kanamycin; Bar: Basta), a red fluorescent protein gene (DsRed, green arrow) that is driven by the seed specific promoter pNAP (orange arrow). Positive selection of recombinant DNA via the *ccdB* gene (red box) that is flanked by the recombination sites *attR1* and *attR2* (white boxes). The part between the left and right border (LB and RB respectively; grey boxes) will be transferred to the plants genome after transformation.

Gateway technology

Primers were designed with the online tool from Invitrogen (www.thermofisher.com) based on sequence information found on the *Arabidopsis* 1001 genomes website. Gateway primers were designed with the following characteristics:

attB1 forward primer: 5' -GGGG-ACAAGTTTGTACAAAAAAGCAGGCT-NN-*template specific sequence*-3'

attB2 reverse primer: 5' -GGGG-ACCACTTTGTACAAGAAAGCTGGGT-N-*template specific sequence*-3'

Genomic fragments were amplified by PCR using the Q5 high-fidelity DNA polymerase from NEB in a Bio-Rad T100 thermal cycler. Q5 high-fidelity DNA polymerase has proofreading function and is suitable for long-range amplification. Reaction components (Table 2) and cycling conditions (Table 3) per gene are provided below:

Table 2: Reaction components PCR and amounts for a single PCR reaction

Component	1x Amount
Milli-Q H ₂ O	30,5 µL
Q5 buffer (5x)	10 µL
dNTP (5 µM)	2 µL
Forward primer (10 µM)	2,5 µL
Reverse primer (10 µM)	2,5 µL
Template DNA	2 µL
Q5 polymerase	0,5 µL

Table 3: Cycling conditions PCR reactions with the temperature (temp) and time per step

Step	Temp	Time
Initial denaturation	98°C	30 sec
Denaturation	98°C	10 sec
Primer annealing	* °C	30 sec
Extension	72°C	** min
Final extension	72°C	2 min
Hold	4°C	infinite

35 cycles

* temperature to be determined for each gene; ** extension time is depending on amplicon length (30 sec. per kb for amplicon lengths up to 6 kb; 50 sec. per kb for amplicon lengths >6 kb)

The optimal primer annealing temperature (*) was determined by a temperature gradient. The extension time (**) used was 2½ minute (30 sec/kb) for *ASN2*, and 6 minutes (50 sec/kb) for *PAH2*, this longer extension time per kb is recommended for products >6kb. PCR products were purified using commercial kits (QIAquick PCR purification kit from Qiagen or NucleoSpin Gel & PCR Clean-up from Bioké) and the obtained DNA concentration was measured with a Nanodrop2000. Hereafter, BP reactions were performed according to the standard protocol from Invitrogen that is provided with the kit. For each reaction 250 ng of purified *attB*-PCR product was used together with 150 ng of *pDONR221* and this mixture was incubated overnight at 25°C in a Bio-Rad T100 thermal cycler. 100 ng of *pEXP7-tet* was used as a positive control for the BP Clonase enzyme mix.

2 µL of BP reaction was used for transformation in *E. coli* TOP10 cells by electroporation and cells were subsequently plated on kanamycin selection plates (50 µg/µL). Single colonies were picked and grown overnight in 5 mL LB (50 µg/µL kanamycin). Plasmids were extracted with a QIAprep Spin Miniprep Kit from Qiagen and subsequently visualised on an agarose gel after restriction enzyme digestion. Correct sized entry vectors were used in the LR reaction (Invitrogen). Equal amounts (150 ng per vector) of entry and destination vector were incubated overnight with the LR Clonase enzyme

mix (Invitrogen) at 25°C. Again 2 µL was used for transformation of *E. coli* TOP10 and cells were plated on spectinomycin selective plates (50 µg/µL).

Colonies were minipreped and vectors were checked for correct digestion fragments after restriction enzyme digestion. The complete inserted DNA fragment was amplified in approximately 1kb long regions with overlap to adjacent regions by PCR with the Q5 high-fidelity DNA polymerase, and subsequently sequenced by GATC Biotech with both primers (**Figure 4**). Sequences of Gateway primers and sequencing primers are listed in **Table S1**. Quality of sequencing results was assessed with Snapgene Viewer (free software version; www.snapgene.com), that shows quality scores of each sequenced nucleotide. Expected allele sequences were extracted from the *Arabidopsis* 1001 genome browser and aligned to the obtained sequence results, using the online webtool from MultiAlin (<http://multalin.toulouse.inra.fr/multalin/>).

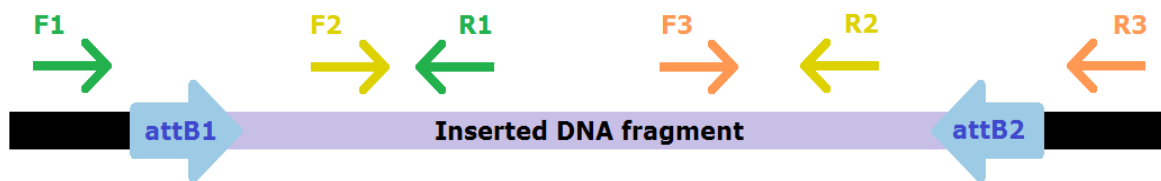


Figure 4: Schematic overview of the position of primers (coloured arrows) designed for sequencing. Primers were designed to amplify regions of about 1000 bp with overlapping ends for alignment and reconstruction of the complete insert.

Gibson Assembly

Gibson Assembly is a cloning strategy that allows for joining of multiple DNA fragments. The different DNA fragments must have ends that are homologous to the adjacent fragment to which they will be combined. During the Gibson Assembly first an exonuclease chews back the 5' ends of each fragment. This allows adjacent DNA fragments to anneal. The 3' ends are extended by a DNA polymerase, and finally a DNA ligase fills the remaining gaps (**Figure 5a**).

Gibson Assembly was used only for cloning of the Ga-0 allele from *PAH2*. During Gibson Assembly multiple DNA fragments can be assembled into one product. The *PAH2* gene was divided and amplified in three fragments: the promoter (2060 bp; fragment 3), ORF (4105 bp; fragment 2) and terminator (922 bp; fragment 1) by Q5 high-fidelity DNA polymerase (NEB) (**Figure 5b**). Primers were designed with Snapgene software (one month trial version) with the Gibson Assembly tool. Primers are designed with the following characteristics from 5' to 3'; 15 to 25 nucleotides that overlap with their flanking region, followed by 18-22 amplicon specific nucleotides. Primer information can be found in **Table S1**.

The expression vector *pKGW_RedSeed* was chosen for molecular cloning of *PAH2*. Since this is a vector suitable for Gateway Technology, the *ccdB* cassette was removed by restriction enzyme digestion (**Figure 5b**). Restriction enzymes were chosen in a way to keep the vector as small as possible for increased transformation efficiency, while maintaining all elements necessary for future steps (LB, RB, selectable marker genes, etc.). Therefore, the expression vector was sequentially cut with *BcuI* (other name for same enzyme is *SpeI*) and *BamHI*, both from Fermentas. All DNA fragments were added in equimolar (1 pmol) concentrations. In order to obtain the high concentrations of PCR fragments necessary to fulfil optimal reaction conditions, multiple PCR reactions per fragment were pooled and subsequently purified with a NucleoSpin Gel & PCR Clean-up from Bioké.

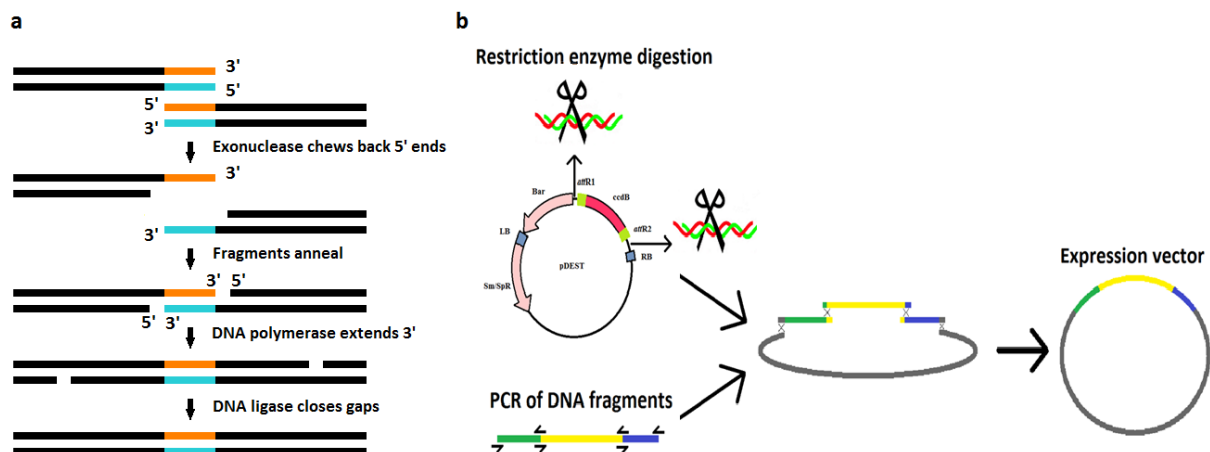


Figure 5: Cloning approach of *PAH2* via Gibson Assembly. **a)** The mode of action of the Gibson Assembly approach. Black lines represent DNA, orange and blue are homologous DNA sequences. **b)** Overview of cloning process of *PAH2*. The Gateway cassette was removed out of the *pBGW* vector by restriction enzyme digestion. The *PAH2* gene was divided amplified was amplified in three PCR fragments: a promoter, ORF and terminator (green, yellow and blue) with homologous ends. Homologous sequences to the cleaved *pBGW* vector were added in the PCR primers that amplified the 5' end of the promoter and the 3' end of the terminator. Fragments were joined in the process described under **a)**.

Also multiple colonies from a glycerol stock with *E. coli* DB3.1 containing the *pKGW_RedSeed* vector were picked and grown overnight in 10 mL LB cultures containing spectinomycin. Overnight cultures were pooled before miniprep. The vector was first digested with *BcuI* (16h at 37°C) after which the linearized vector was extracted from gel because *BcuI* cannot be heat inactivated and has restriction sites in the other fragments. Hereafter the product was digested with *BamHI* (16h at 37°C) and heat inactivated (20 min at 80°C). The four fragments (PCR fragments and vector backbone) were incubated at equimolar amounts with the Gibson Assembly mix (NEB) for one hour at 50°C and subsequently transformed by electroporation into *E. coli* TOP10. Colonies were picked, grown overnight in liquid LB medium containing antibiotics and miniprepped. Products from the miniprep were digested with *NdeI* (16 hours at 37°C) and checked for correct restriction fragments.

Generation of the triple mutant *asn2-1pah1pah2*

pah1pah2 (SALK_042850 x SALK_047457) was crossed to *asn2-1* (SALK_043167). Offspring were selfed and subsequently genotyped. DNA was isolated from a single young leaf using the CTAB DNA extraction protocol (*Supplemental data, Protocols, CTAB DNA extraction*). Presence or absence of T-DNA insertions inside the three genes were visualised on 1% agarose gels after PCR with GoTaq polymerase from Promega. Suggested protocol and cycling conditions by the manufacturer were used with a melting temperature of 54°C for all primers (**Table S1**). Extension time was amplicon specific adjusted to 1 kb/min. Genotyping for *ASN2* was done by separate PCR reactions for detection of WT allele or T-DNA insertion. For both *PAH1* and *PAH2* genotyping was done in a single PCR reaction with all the three primers.

Light experiment

Set up

Seeds were incubated for 2 days at 4°C for uniform germination. After this, they were individually sown on rock wool blocks from Grodan in the climate chamber (D2) under four different light intensities; 100, 200, 400 and 550 $\mu\text{mol photons m}^{-2} \text{s}^{-1}$. The highest light intensity, 550 $\mu\text{mol photons m}^{-2} \text{s}^{-1}$, was achieved by full exposure to the light present in the growth chamber. To create the other light intensities, a PVC construction around each light department was built. Layers of cloth were placed around each of these constructions, with more layers of cloth for the compartments with a lower light intensity. The number of cloth layers were determined using a light meter, with increasing layers until the correct light intensity was reached. For the lowest light intensity two different kinds of cloth were used in order to reach sufficient blocking of the light. Rock wool blocks were placed in plastic trays for watering within each compartment. On each rock wool block, a black round rubber was placed with a small hole in the middle, in which one seed was sown. This black rubber was used for having a uniform background for the photosynthesis measurements, which also circumvents measurement errors in the chlorophyll fluorescence imaging caused by algae growing on the rock wool blocks. Genotypes that were tested are COL-0, *asn2-1*, *pah1*, *pah2*, *asn2-1/pah1*, *asn2-1/pah2*, *pah1/pah2*, *asn2-1/pah1/pah2* and the natural accessions Ga-0 and Ts-1. Plants were grown continuously in the same light intensity during the day with 12 hours of light (08:00 to 18:00) at 70% humidity. Also six plants per genotype were transferred from 100 to 550 $\mu\text{mol photons m}^{-2} \text{s}^{-1}$ at 25 days after sowing.

Measurements of growth

Photographs were taken from the same two plants per genotype (Col-0, *asn2-1*, *pah1pah2*, *asn2-1pah1pah2*, Ts-1 and Ga-0) from plants that were the largest and strongest looking in the beginning of the experiment. This size selection was done in order to enlarge the probability that the particular plants would survive during the whole experiment. The photographs were taken with a Nikon D3000 at 19, 21, 23, 26 and 29 days after sowing. The camera was put on a standard that stayed on the same position during the whole experiment, and the settings of the camera were kept constant (manual mode; F-stop: f/5.3, ISO: iso-200; exposure time: 1/250 sec). These photographs were analysed by ImageJ software with the Measure rosette area plugin from the Remote-ImageJ project (<http://dev.mri.cnrs.fr/projects/remote-imagej/files>; filename: *Macro_IO_settings*). Standard settings were used from this plugin except: minimal luminosity was set to "125" and maximal luminosity to "275" in order to detect the complete rosette. ImageJ then counted the number of pixels that make up the rosette. The zoom of the camera was not constant during the whole experiment. On the first day of measurement, with small plants, higher magnification was applied compared to later during the experiment when the whole rosette was not captured anymore on the photograph. Therefore, a correction factor was applied to the data obtained from ImageJ. The background of the camera holder had a centimetre grid on the bottom. Via ImageJ the number of pixels of a perfect horizontal line of 10 cm was measured for one photograph per measurement day (the magnification did not change within a measurement day). The rosette area calculated by ImageJ was normalised by dividing the number of pixels (measured by ImageJ) by the number of pixels that are 10 cm of the grid. Fresh weight was measured from whole plants at the end of the experiment using a balance (Mettler Toledo New Classic MS204s).

Chlorophyll fluorescence imaging

The efficiency at which light is used by the photosynthetic apparatus can be measured by chlorophyll fluorescence imaging (CFI). Chlorophyll fluorescence was measured with a Fluorcam 7 (<https://www.psi.cz>) from Horticulture and Plant Physiology. Plants were taken from climate chamber D2 and transferred to the Fluorcam for CFI measurements. Measurements were taken for plants that moved from low to high light intensity at 25, 26, 27, 29 and 33 days after sowing. For all other plants that remained in their respective light environment the measurements were taken at 33 days after sowing. For each CFI measurement three biological replicates per accessions are used.

Quantitative real-time PCR (qRT-PCR)

Whole rosettes (3 replicates per genotype) were harvested at 25 days after sowing ($100 \mu\text{mol photons m}^{-2} \text{s}^{-1}$) and at 26 days after sowing ($550 \mu\text{mol photons m}^{-2} \text{s}^{-1}$), both at 11.00h am, from plants that had been transferred the evening before from low to high light intensity. Samples were immediately frozen in liquid nitrogen. RNA was isolated from grinded plant material with an automatic grinder (Retsch MM300) according to the DNA-free RNA isolation protocol (*Supplemental data, Protocols, RNA isolation*). RNA concentration and quality was measured with a Qubit 2000 and diluted to 200 ng/ μL . cDNA was synthesised using Iscript cDNA synthesis kit from Bio-RAD (*Supplemental data, Protocols, cDNA synthesis*). qRT-PCR was performed on three technical replicates per biological replicate (*Supplemental data, Protocols, qRT-PCR*), using SYBR-green mastermix from Bio-RAD. Reference genes *UBQ7* (AT2G35635) and *CB5E* (AT5G53560) were used for normalisation (**Jung et al. 2013**) (**Wunder et al. 2013**). From each genotype representative and similar looking plants were chosen when possible. qRT-PCR primers were designed with the online Primer3Plus software based on sequence information from the *Arabidopsis* 1001 genome browser, with amplicon lengths between 80-130 bp and maximal 0.5°C difference in T_m . Primer efficiencies were determined based on the slope of a standard curve, obtained by performing qRT-PCR on a series of diluted cDNA samples (0x, 2x, 4x and 8x dilutions of cDNA). The efficiency was automatically calculated by Bio-Rad CFX Manager 3.1 software, primers used all had efficiencies between 90% and 105%. Melting temperature curves were checked for all primer pairs, and had to give a single and distinct peak for all samples. Multiple primer melting temperatures are indicative of aspecific amplification or primer dimerization.

Samples that gave no results (because of failed RNA extraction) or gave results that differed to a very large extent compared to biological replicates for expression of (nearly) all genes were removed in all datasets. Therefore, all datasets contain the same number of biological replicates. Single technical replicates were removed when no, or double amounts of cDNA was added by accident. All primer sequences and T_m are in **Table S1**. Expression values are calculated using a delta Ct method. The average C_q value of the two references genes was subtracted from the average of three technical replicates of each biological sample, which gives the delta Ct value. The expression was then calculated as $2^{-\text{Ct}}$.

Statistics

For comparison of qRT-PCR data, two sided t-tests (two tailed) were performed in Excel between delta Ct values. T-tests on delta Ct values were performed within a genotype but between two light treatments, and between two genotypes (Col-0 and any other genotype) within the same light treatment. Two sided t-tests (two tailed) were also performed for each ϕPSII data point, with

comparisons between Col-0 and different mutant lines. Dry weight data was analysed with a Tukey test in SPSS software for every available genotype within the same light condition.

Results

Molecular cloning

To do an allelic complementation test, the high alleles of *ASN2* and *PAH2* have to be cloned. It is not known if the epistatic interaction is based on expression or protein differences. Therefore, the entire allele are cloned with their endogenous promoter and terminator included. Primers are designed on positions directly bordering the adjacent up- and downstream genes (**Figure 2**). The expected total size of the *ASN2* allele is 4193 and 6851 bp for the *PAH2* allele.

Multiplication of vectors

Vectors (*pDONR221*, *pBGW* and *pKGW_Redseed*) were multiplied in a previously prepared stock of *E. coli* DB3.1. This yielded approximately 20 colonies for *pDONR221*, only one colony for *pBGW* and only three colonies for *pKGW_Redseed*. Ten random colonies from *pDONR221* were digested by *NruI* and a combination of *NruI* and *EcoRI*; the *pBGW* colony was digested by *NdeI* (**Figure 6a**) and *EcoRI* (**Figure 6b**), and the *pKGW_Redseed* colonies by *EcoRI* (**Figure 6a**). All colonies showed correctly sized restriction fragments, and glycerol stocks were prepared. Later during the experiments multiplication of *pDONR221* was repeated because sequencing had revealed a small deletion in one of the samples inside the *ccdB* cassette. Because the BP reaction during Gateway cloning was very difficult, the *pDONR221* samples were discarded and new vectors were amplified with a fresh stock of *E. coli* DB3.1 and a new vector stock from a different department. Simultaneously, also *pDONR201* was multiplied because stocks had ran out at our lab, but this vector was not further used during this project. From this new *E. coli* DB3.1 stock about 50-100 colonies grew per transformation, of which ten colonies were randomly picked per vector and digested (**Error! Reference source not found.**). All ten colonies harbouring *pDONR221* showed correct digestion patterns, and four out of ten correct digestion patterns for *pDONR201*.

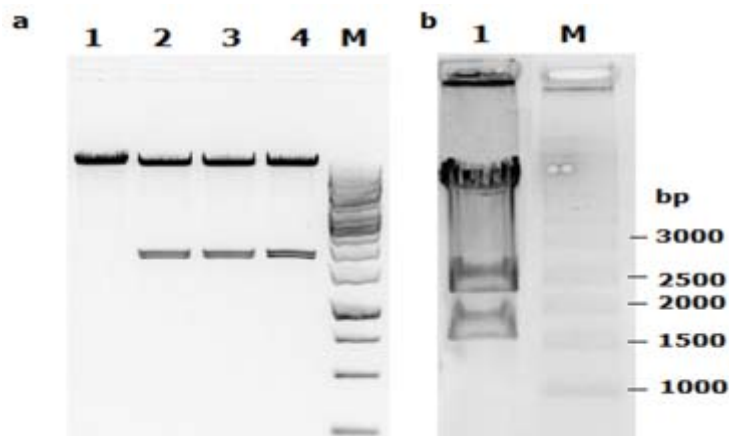


Figure 6: a) Digestion of *pBGW* (lane 1) and *pKGW_Redseed* (lane 2-4) with *NdeI*. Expected sizes of digestion fragments: lane 1: 9669 bp; lane 2-4: 9421 bp, 1681 bp and 1596 bp. The marker lane is not reliable because of prestaining by Gel Red. **b)** Digestion of *pBGW* with *EcoRI*. Expected sizes of restriction fragments: 5447 bp, 2489 bp and 1733 bp.

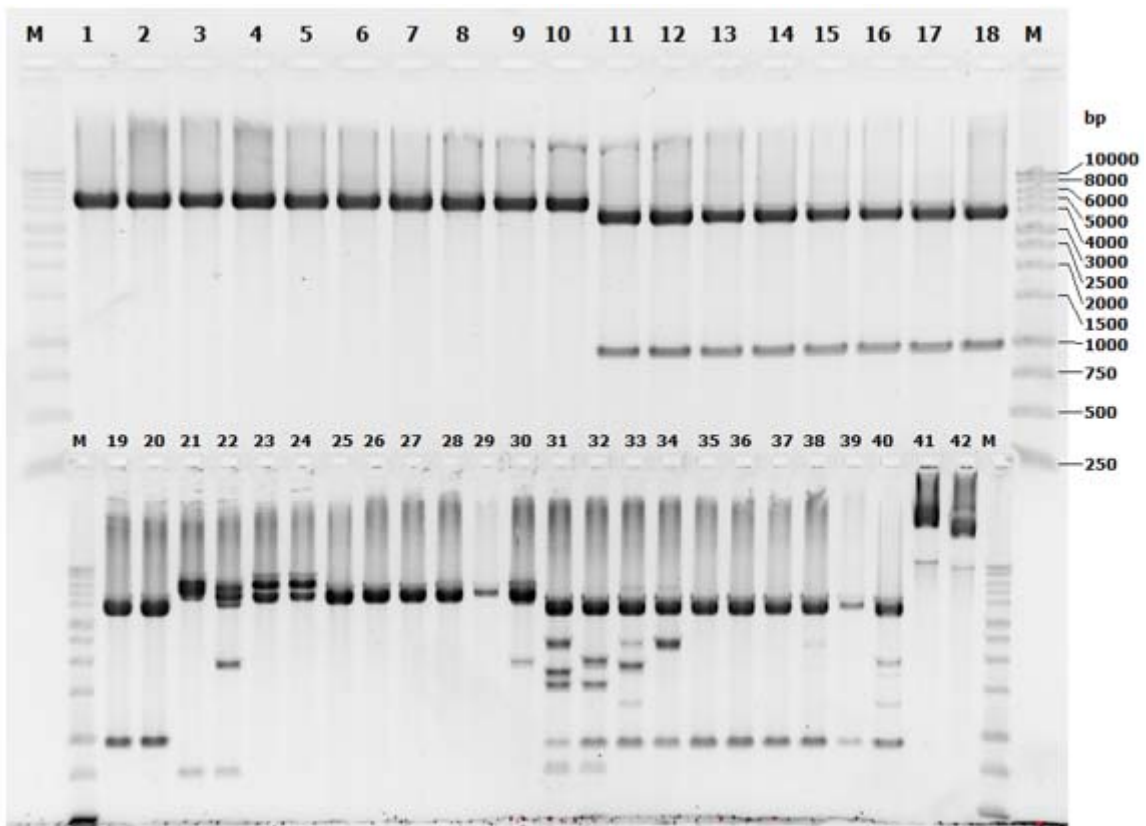


Figure 7: Restriction enzyme digestion of *pDONR221* (lane 1 – 20) and *pDONR201* (lane 21 – 40). Each of the ten samples per plasmid were digested with *NruI* and *NruI + EcoRI*: lane 1 and lane 11, lane 2 and lane 12 etc. contain the same plasmid. Lane 1 – 10: *pDONR221 + NruI* (expected size: 4763 bp); lane 11 – 20: *pDONR221 + NruI + EcoRI* (expected sizes: 948 bp and 3814 bp); lane 21 – 30: *pDONR201 + NruI* (expected size: 4470 bp); lane 31 – 40: *pDONR201 + NruI + EcoRI* (expected sizes: 901 bp and 3569 bp). All *pDONR221* show correct sized digestion patterns, while four out of ten digestion patterns are correct for *pDONR201*.

Gateway technology

Genomic DNA was isolated from young single leaves, originating from different biological replicates. In the first attempt to amplify the genomic regions of both genes, the suggested primer melting temperatures (T_m) were first tested ($T_m=59^\circ\text{C}$). For *ASN2* this gave aspecific products for all four different DNA samples (**Figure 8a**) while for *PAH2* no product was seen. For *ASN2* the T_m was increased to 63°C , while for *PAH2* a temperature gradient from 60°C (lane 1) to 65°C (lane 6) was applied (**Figure 8b**). Both genes gave optimal amplification without aspecific products at $T_m=63^\circ\text{C}$ (**Figure 8c**).

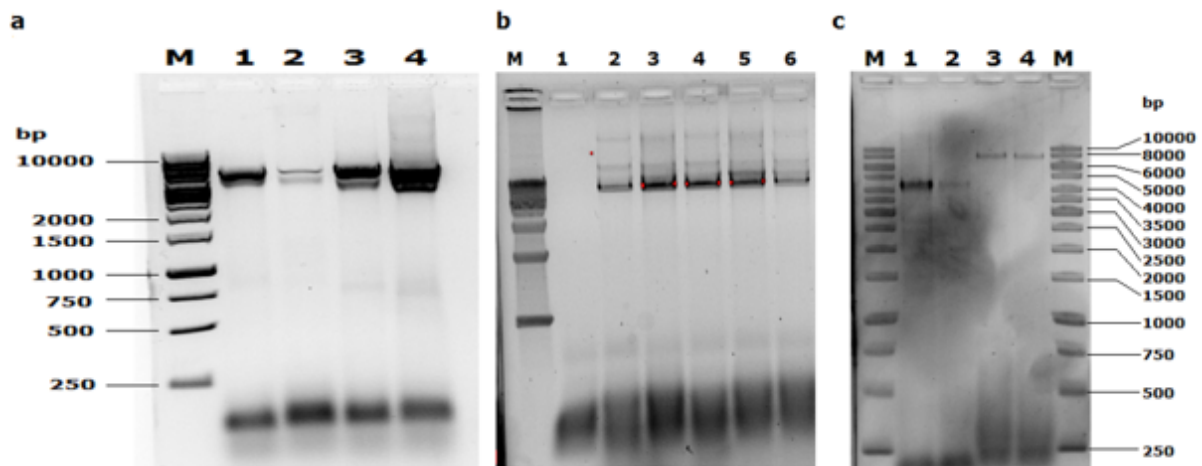


Figure 8: a) Amplification of *ASN2* at $T_m = 59^\circ\text{C}$ for four different Ga-0 gDNA samples (lane 1-4). b) Gradient PCR on *PAH2*, T_m ranging from 60°C (lane 1) to 65°C (lane 6). c) Amplification of both *ASN2* (lane 1 & 2) and *PAH2* (lane 3 & 4) at $T_m = 63^\circ\text{C}$.

Although in **Figure 8c** the *PAH2* PCR product in lane 3 and 4 the PCR shows acceptable results, amplification of *PAH2* was often problematic and gave quite high amounts of primer dimers (**Figure 8b**). This PCR was especially sensitive to the quality of the DNA template, and for most of the different DNA samples no amplification could be obtained for *PAH2* while the same DNA samples gave strong results for *ASN2* amplification.

Several factors have been tested in an attempt to increase the amount of product; increasing and decreasing the amount of template DNA (0.5x and 2x), dilutions of template DNA (2x and 4x dilutions), increasing and decreasing primer concentrations (0.5x and 2x), increasing dNTPs (2x), increasing and decreasing amount polymerase (0.5x and 2x). All these attempts were made with DNA samples known to amplify *PAH2*. Furthermore the extension time in the PCR cycle was increased up to 60 sec/kb. None of these changes showed improvements of total amount of product, and often no amplicon could be detected with the changes. Another pair of primers was tested with a temperature gradient ($59^\circ\text{C} - 66^\circ\text{C}$) but this pair of primers showed very high primer dimerization (**Figure 9**).

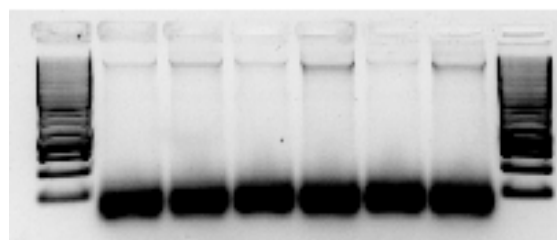


Figure 9: Temperature gradient ranging from 59°C to 66°C for PCR of *PAH2* with alternative primers showing low amount of amplicon and high amount of primer dimers in all lanes.

For both genes multiple PCRs were pooled, purified, used in the BP reaction and subsequently transformed in *E. coli* TOP10 and plated on selective medium. In this first attempt the selection plates were completely covered with small colonies; miniprepping these colonies revealed that they were all false positives, with no vectors being recovered. Either the used antibiotic was not working (antibiotic too old, plates poured too hot) or the plate was not dried long enough after inoculation. In the second attempt new selection plates were made and two extra controls were added to test if the antibiotic was effective; one LB plate with (+) and one without (-) antibiotics (kanamycin). Both plates

were 'inoculated' by touching them with bare, 'dirty' hands. The new control plates showed that the antibiotic was working (several different kinds of colonies grew on the LB- touched with 'dirty' hands, but no bacteria grew on the LB + plate with 'dirty' hands). In this new attempt, about 15 colonies grew for *ASN2* and 5 colonies for *PAH2*. An agarose gel with the obtained miniprep products from these colonies showed that none of the colonies had correct plasmids (almost all empty vectors).

In the third attempt with again a new BP reaction, six colonies for *ASN2* (Ga-0 allele), and five colonies for *PAH2* (Ga-0 allele) had grown. After miniprep this number was further reduced to four and two (*ASN2* and *PAH2* respectively) potentially correct ones. These samples were digested with *EcoRI*, which would give one expected band of 6741 bp for *ASN2* entry clones and four bands for *PAH2* entry clones of 9226, 665, 158 and 48 bp (**Figure 10**). As a control *pDONR221* was digested which would give a 4762 bp band, and *pKGW_Redseed* was added to test if *EcoRI* digestion was successful (9421, 1681 and 1596 bp bands). Only lane 2 (**Figure 10**) (*ASN2* Ga-0 allele) seemed based on size a potentially correct entry clone. Lane 1, 3, 4 and 6 were of the same size as *pDONR221*, suggesting a complete *pDONR221*. Lane 2 was followed up by *NruI* digestion which showed correct restriction fragments (3714, 3027 bp; figure not shown). Furthermore insertion of *ASN2* was checked by PCR by using the original primers to amplify *ASN2*, which gave good amplification of the insert. Therefore, this entry vector was used in the LR reaction together with the vector *pBGW*. Transformation yielded four colonies which were miniprepped and put directly on gel (expected size 12230 bp) (**Figure 11a**) and digested with *NcoI* (expected sizes 8303 and 3908 bp) (**Figure 11b**). All four colonies gave correct digestion patterns.

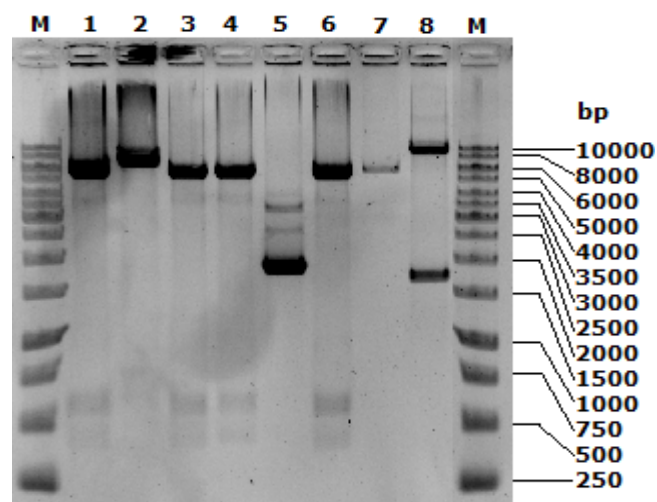


Figure 10: Restriction pattern of possible entry clones when digested with *EcoRI*. Lane 1 – 4: possible *ASN2* clones (expected size: 6741 bp); lane 5 & 6: possible *PAH2* entry clones (expected size: 9226 bp, 664 bp, 158 bp and 48 bp). Lane 7: *pDONR221* + *EcoRI* (expected size: 4761 bp). Lane 8: *pKGW_Redseed* + *EcoRI* (expected size: 9421 bp, 1681 bp and 1596 bp).

The inserted *ASN2* allele was sequenced for colony #1 by ten sequencing reactions. The inserted sequence from *ASN2* plus a small part both upstream of *attB1* and downstream of *attB2* was divided into five regions of about 1000 bp of which the ends were overlapping with neighbouring regions (**Figure 4**). Primers were chosen to have a similar T_m of about 60°C. In the first attempt, all five PCRs gave good amplification without aspecific products (**Figure 11c**) and were sent for sequencing with both the forward and reverse primer in separate sequencing reactions.

Per fragment the sequencing results obtained from the forward primer and the reverse complement of the reverse primer were aligned. In case of a SNP between these two alignments, the quality of the sequence at that particular locus was assessed for both sequencing results to determine the most likely correct nucleotide. Next, all five regions were joined to obtain the full length sequence of the *ASN2* Ga-0 insert, which was aligned to the expected sequence based on the *Arabidopsis* 1001 genome browser. In total, five differences were present in the construct (**Figure 12**): two SNPs that might possibly be in the promoter region (-586 bp and -570 bp upstream of the start codon), a 4 bp deletion and one SNP in the region downstream of the terminator (the deletion at 408 bp downstream of stop codon, the SNP at 419 bp downstream of the stop codon). This 4bp deletion and SNP fall inside *At5g65015* which was partially included in the vector because no other suitable primers could be designed that would also capture the whole terminator region. Finally one SNP in an intron between exon 8 and 9 (32 bp downstream from the 3' end of exon 8 and 61 bp upstream of the start of exon 9).

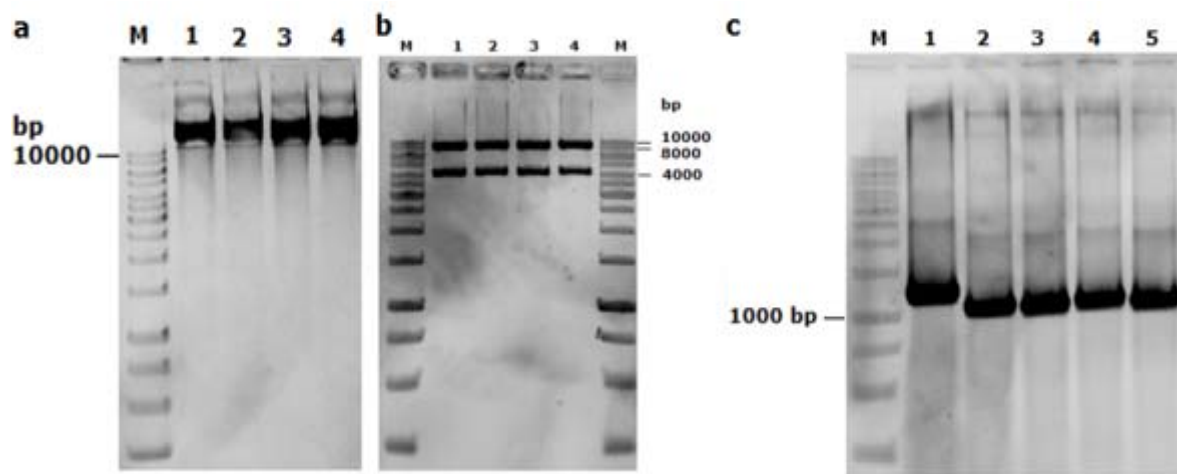


Figure 11: a) Possible correct *pBGW::ASN2*(Ga-0) expression vectors put directly on gel from four colonies (expected size: 12230 bp). b) The same four samples as in (a), digested with *NcoI* (expected sizes: 8303 bp & 3908 bp). c) Amplification of five PCR reactions on *pBGW::ASN2*(Ga-0) colony #1 used for sequencing (expected sizes: lane 1: 1152 bp, lane 2: 997 bp, lane 3: 985 bp, lane 4: 1001 bp, lane 5: 965 bp).



Figure 12: Map of sequence differences between Col-0, Ga-0 and the *pBGW::ASN2*(Ga-0) construct. The top lane shows exons/introns of *ASN2* (*At5g65010*; from the 1001 *Arabidopsis* genome browser). In the third and fourth lane sequence differences compared to Col-0 (second lane) are depicted with coloured stripes and a nucleotide code. The small purple bar in the Vector (fourth) lane on the right side represents a 4 bp deletion.

The fourth attempt of cloning *PAH2* via Gateway gave about 100-150 colonies. 95 colonies were picked randomly and tested by colony PCR with primers that would amplify a small fragment of the *PAH2* insert. The vast majority of these colonies gave the same band as the positive control, but no negative control was added. 80 colonies were miniprep and the concentrations of DNA were measured by a Nanodrop 2000. All miniprep reactions showed low yield (between 20-50 ng/ μ L) of DNA, which was already indicative of false positive colonies. Colonies that harbour vectors after transformation nearly always give concentrations of at least >100 ng/ μ L after miniprep of a 5 mL LB overnight culture. In practice colonies that give concentrations <80 ng/ μ L were always false positives, and genomic DNA was isolated. This was also the case for all the 80 tested colonies; none of them gave any band in the right range of size of a possible correct vector. Therefore the colony PCR was repeated with only three random colonies and a negative control. This negative control gave the same product with the same intensity, thus showing that most likely one of the pipets was contaminated.

Gibson assembly

Cloning of *PAH2* was continued by Gibson Assembly (**Figure 5**). Amplification of the three fragments gave no problems and succeeded at first attempt (**Figure 13a**). In the first Gibson Assembly attempt, 0.2 pmol per fragment was added (115 ng fragment 1; 250 ng fragment 2; 500 ng fragment 3; 1 μ g vector backbone). After electroporation no colonies were present. Two positive controls were performed in order to assess if the failed Gibson Assembly was due to loss of competence of the electro competent cells or loss of functionality of the Gibson Assembly master mix. *E. coli* TOP10 cells were therefore transformed with *pUC19* and a positive control from the Gibson Assembly kit. *pUC19* was used before to test competence of the same batch of electro competent cells. The positive control from the Gibson Assembly kit consists of two linear DNA fragments on which a functional antibiotic resistance gene (ampicillin resistance) is formed when the two fragments are assembled correctly. A high number of colonies would be expected in case the cells were still competent, and the mastermix was still working correctly. The *pUC19* control showed that cells were still very competent while the positive control from the Gibson Assembly yielded a very low number of colonies.

Therefore, in a second and last attempt to clone *PAH2* (Ga-0) a new Gibson Assembly master mix was used. Furthermore the molar concentrations of all fragments were increased from 0.2 pmol up to 1.0 pmol per fragment (6.2 μ g vector backbone, 570 ng fragment 1, 2.5 μ g fragment 2, and 1.25 μ g fragment 3). Since the total volume of the fragments was only 10 μ L, especially for the vector backbone a very high concentration had to be achieved. To achieve this, the glycerol stock with the *pKGW_Redseed* vector was used to plate single colonies. 15 colonies were picked and were each grown in 10 mL LB medium. During miniprep, overnight cultures were pooled into three aliquots (thus each containing 5 overnight cultures). These were separately digested and put on gel. During gel extraction, the three different samples were pooled again and dissolved in 15 μ L, resulting in a final concentration of 2 μ g/ μ L.

After one hour incubation of the four fragments with the Gibson Assembly mastermix and transformation, about 80 colonies grew of which 46 random colonies were put on a new plate and tested by colony pcr (**Figure 13b**) with primers that would amplify an approximately 800 bp fragment inside the ORF of *PAH2*. Genomic DNA from a Ga-0 plant was used as a positive control, while in the negative control no DNA was added. This control was performed in order to assess possible contaminations in for example a pipette that were seen in a previous colony PCR. In total 39 colonies

showed a similar result to the positive control. 20 colonies of these were grown overnight and 18 of these were minipreped (two did not grow) and digested with *NdeI* (**Figure 14**). The digestion pattern of correct vectors would be: 6478 bp, 6149 bp, 2489 bp and 1733 bp. In **Figure 14**, lane 4, 8 and 11 to 16 show this pattern although the 6478 and 6149 bp band are not distinguishable. The combination of [1] being able to grow on selective medium (solid and liquid LB with antibiotics), [2] correctly sized band in the colony PCR and [3] a seemingly correct digestion pattern indicates that these are correct vectors. From these eight colonies glycerol stocks are made, but the vectors have not yet been sequenced.

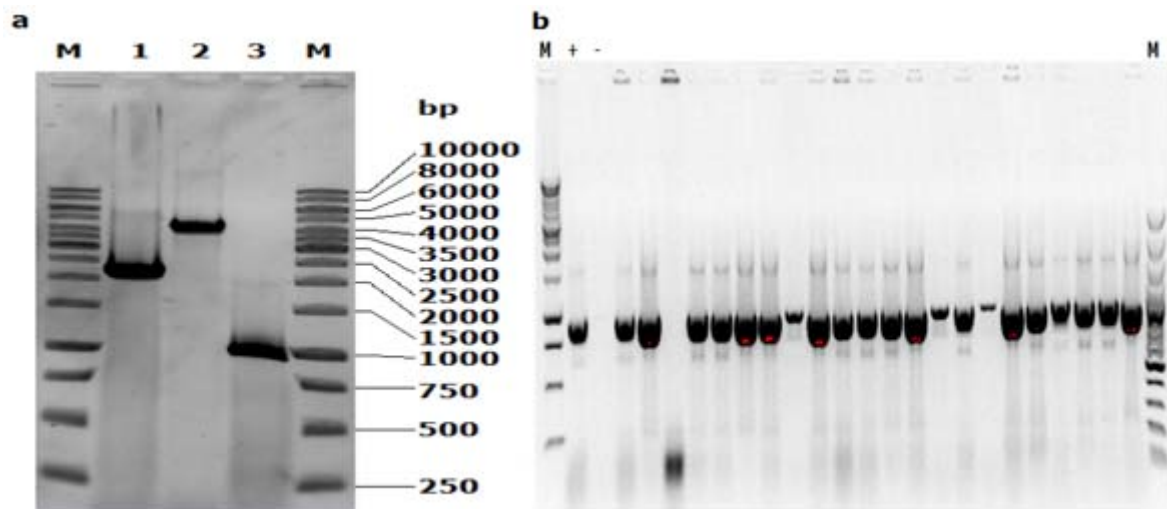


Figure 13: a) PCR results of three *PAH2* Ga-0 Gibson Assembly fragments. Lane 1: fragment 3 (promoter region, expected size: 2060 bp); lane 2: fragment 2 (ORF, expected size: 4105 bp) and lane 3: fragment 1 (terminator, expected size: 922 bp). b) Colony PCR on random picked colonies harbouring possible correct *pKGW_Redseed::PAH2(Ga-0)* expression vectors. Genomic DNA was added to the positive control (+ lane) while no DNA/bacteria were added to the negative control (- lane).

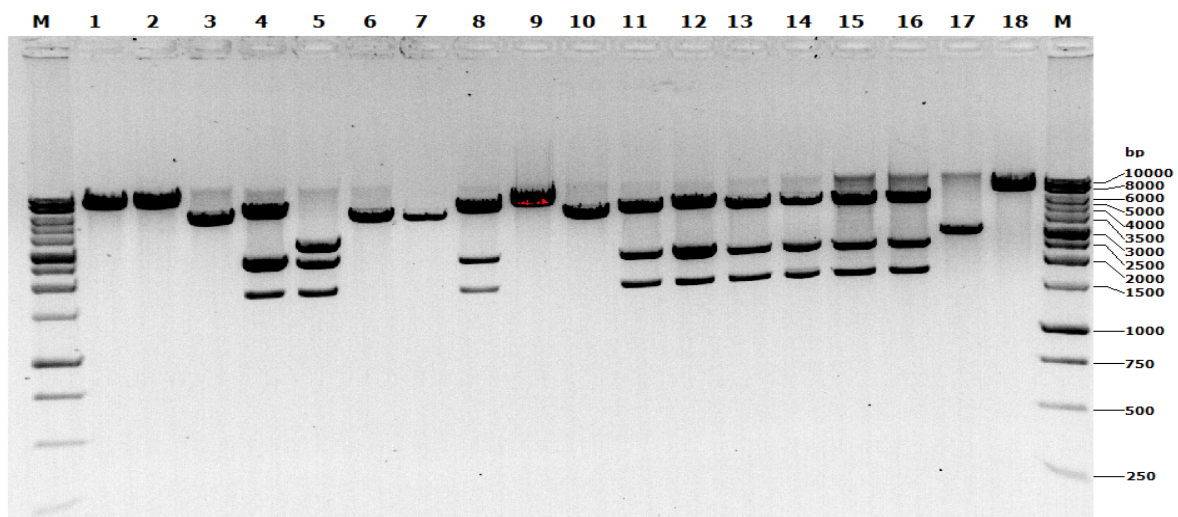


Figure 14: Restriction enzyme digestion of possible *pKGW_Redseed::PAH2(Ga-0)* expression vectors. Expected sizes for correct vectors are 6478 bp, 6149 bp, 2489 bp & 1733 bp.

Generation of the triple mutant *asn2-1pah1pah2*

An *ASN2asn2PAH1pah1PAH2pah2* was selfed and seeds were collected. 192 plants were sown of which 182 plants germinated and were genotyped by PCR for these three genes. 1.56% of all offspring was expected to be a triple mutant, that would be two to three plants. Genotyping revealed that no triple mutants were present. Therefore, in order to increase the likelihood of finding a triple mutant, two plants from this progeny with genotypes *ASN2asn2pah1pah1pah2pah2* were selfed. Per selfing 48 seeds were sown and genotyped. The results showed that a mistake was made in selection of one of the parents, since there were still heterozygotes present for *PAH2* in the offspring, showing that the genotype of one of the parents was *ASN2asn2pah1pah1PAH2pah2* instead. Five out of the first 23 plants were triple mutants, see as an example **Figure 15**. These plants were used to yield seeds for further experiments. The triple mutant was pale green, similar to *asn2-1*, see **Figure 16**.

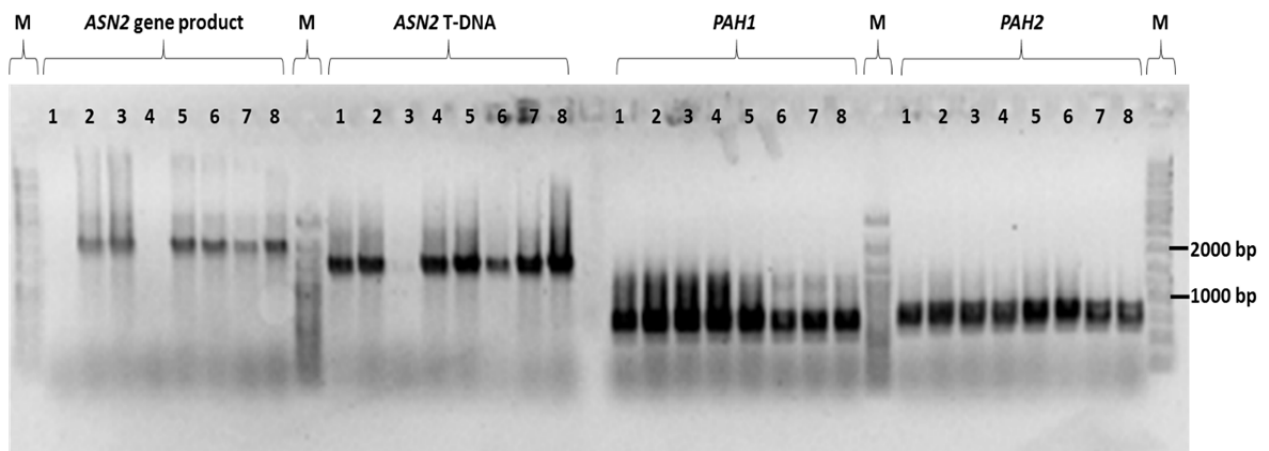


Figure 15: Example of genotyping of eight plants. PCR products of the same eight plants loaded from #1 to #8 for all four genotyping PCR reactions. All plants are homozygous the T-DNA insertion in both *PAH1* and *PAH2* (expected size: ~600 bp while wild type Col-0 fragment would be ~1100 bp). Plant #1 and #4 are triple mutants.

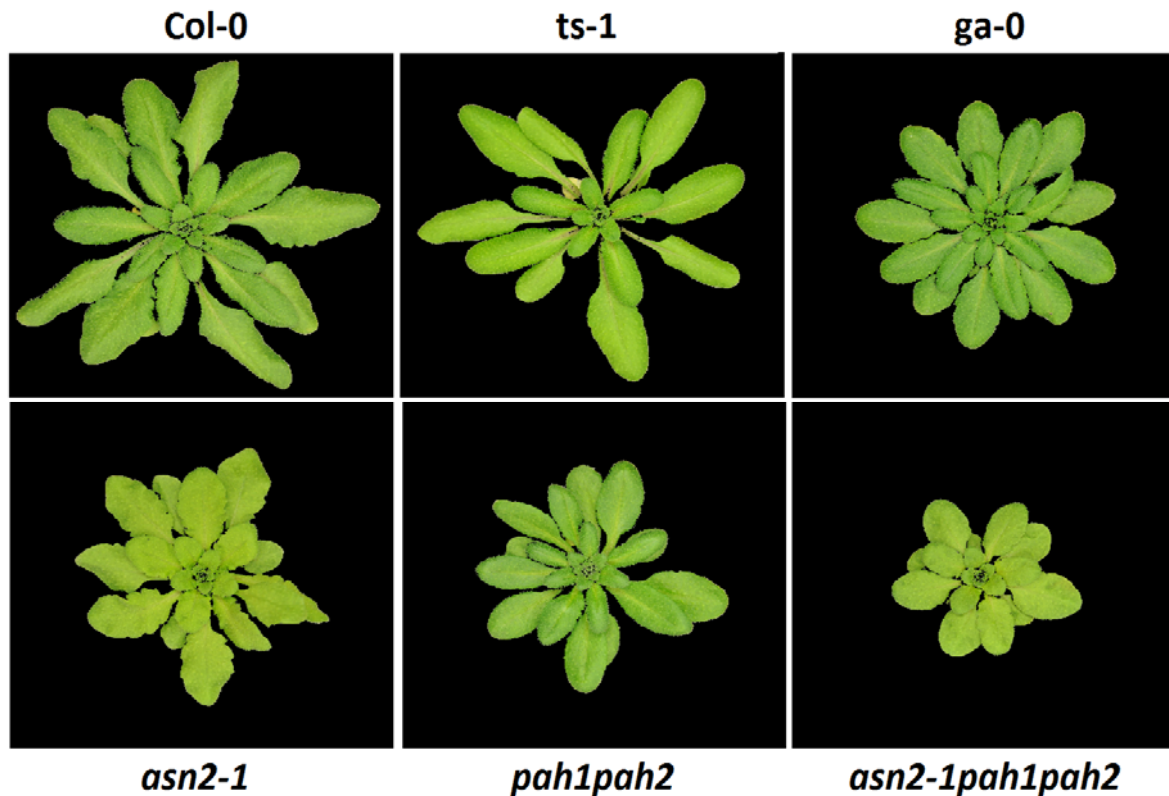


Figure 16: Phenotypes of the different accessions and mutant lines grown under a light intensity of $500 \mu\text{mol photons m}^{-2} \text{s}^{-1}$ 27 days after sowing. Although difficult to see on this figure, the triple mutant was pale green, similar to *asn2-1*.

Light experiment

Plant growth

Pictures of two plants were taken to get an indication of the effect of the epistatic interaction on plant growth. The same two plants per genotype were followed over a period of 10 days by photographing them at 19, 21, 23, 26 and 29 days after sowing. Due to time constraints only two replicates per genotype were manually photographed.

Some of these plants died before the end of the experiment. Only in case of the triple mutant at $100 \mu\text{mol photons m}^{-2} \text{s}^{-1}$ both plants died before the end of the 10 days. The photographs were analysed by ImageJ software which counted the number of pixels that make up the rosette (**Figure 17**). The analysis is based on the colour values of each pixel, and did not always provide reliable results. This was the case when plants were very small and pale looking, or when plants were very large and one of the leaves would 'touch' the outside of the photograph. This latter case would give huge overestimations. The analysis was run with the same settings for all photographs and the results were checked carefully one by one. Unreliable results were removed. Growth of single rosettes per genotype under the four different light intensities are shown in **Figure 18**. When any genotype is phenotyped under the four different light intensities, it is clear that plants grow larger with increasing light intensity. Furthermore, the triple mutant is most affected in its growth under all light intensities. Ts-1 seems to perform best under the two lower light intensities however because growth is only shown for single plants per genotype, no real conclusions can be drawn out of these results, even though the plants analysed here appeared to be representative.

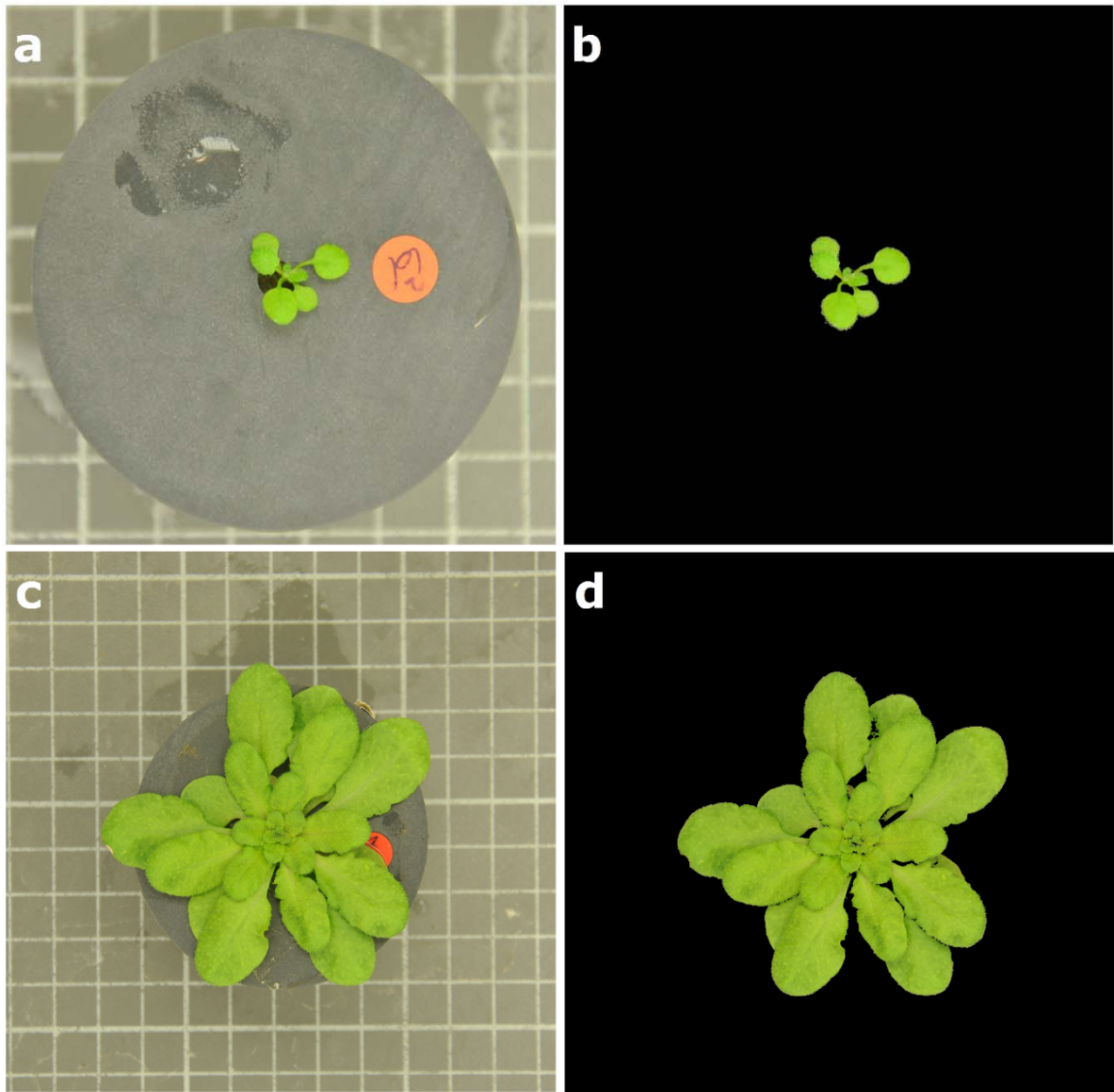


Figure 17: Example of analysis by ImageJ software. A Col-0 plant 19 days after sowing grown at $100 \mu\text{mol photons m}^{-2} \text{s}^{-1}$ (a and b); and a triple mutant 29 days after sowing at $550 \mu\text{mol photons m}^{-2} \text{s}^{-1}$ (c and d).

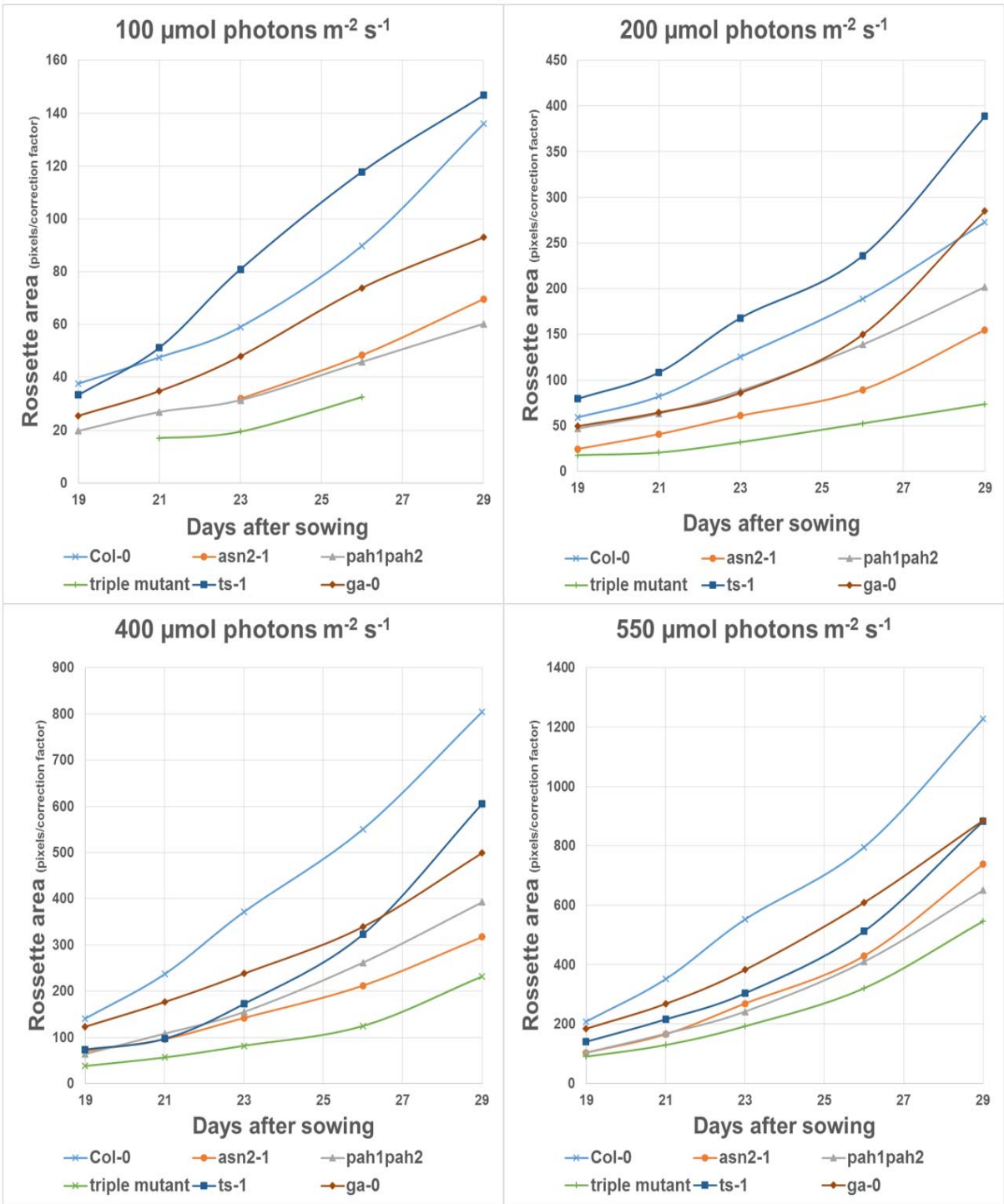


Figure 18: Growth of single rosettes during ten days of the light experiment under 100 (a), 200 (b), 400 (c) and 550 (d) $\mu\text{mol photons m}^{-2} \text{s}^{-1}$. Data points for the triple mutant are missing in (a) because the software was not able to accurately measure the size, while the last data point is missing because the plant died.

The fresh weight was measured at the end of the light experiment for the remaining plants of each genotype, see **Figure 19**. A Tukey test was performed on the fresh weight of the different genotypes in each light treatment, see **Table S2**, **Table S3**, **Table S4** and **Table S5**. Under 100 $\mu\text{mol photons m}^{-2} \text{s}^{-1}$ no significant differences were seen between genotypes although the triple mutant and Ts-1 were not measured (Ga-0 is also missing), while in **Error! Reference source not found.** these two were the most extreme genotypes. Under the other light intensities a quite similar pattern is seen as in **Figure 18**, with the triple mutant having the lowest weight, while Ts-1 (200 $\mu\text{mol photons m}^{-2} \text{s}^{-1}$) and Col-0 (400 and 550 $\mu\text{mol photons m}^{-2} \text{s}^{-1}$) having the highest weight. The weight of the triple mutant was lower compared to Col-0, Ga-0 and Ts-1 under the three measured light intensities. However, when the first generation of triple mutants was grown in another climate chamber (C14), most triple mutants were clearly larger than either the *asn2*, *pah1pah2* or reference accession Col-0 **Figure 20**. In this climate chamber both Col-0 and *asn2*, but not *pah1pah2* and the triple mutant, showed signs of stress with anthocyanin accumulation (purple colouration) on the abaxial side of the leaves. This abaxial purple colouration was not observed in the Col-0 plants from the D2 experiment.

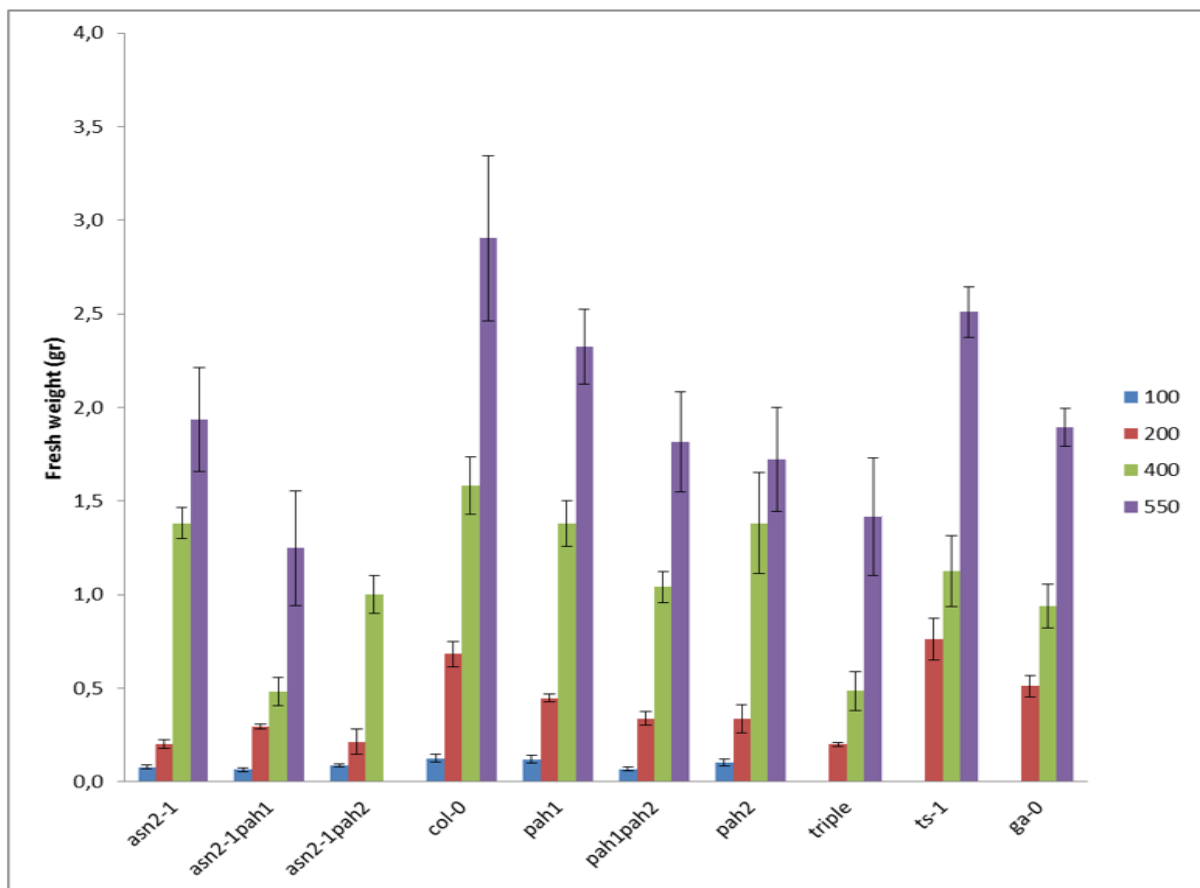


Figure 19: Fresh weight of the different accessions and mutants under 100, 200, 400 and 550 $\mu\text{mol photons m}^{-2} \text{s}^{-1}$. Error bars are SE.

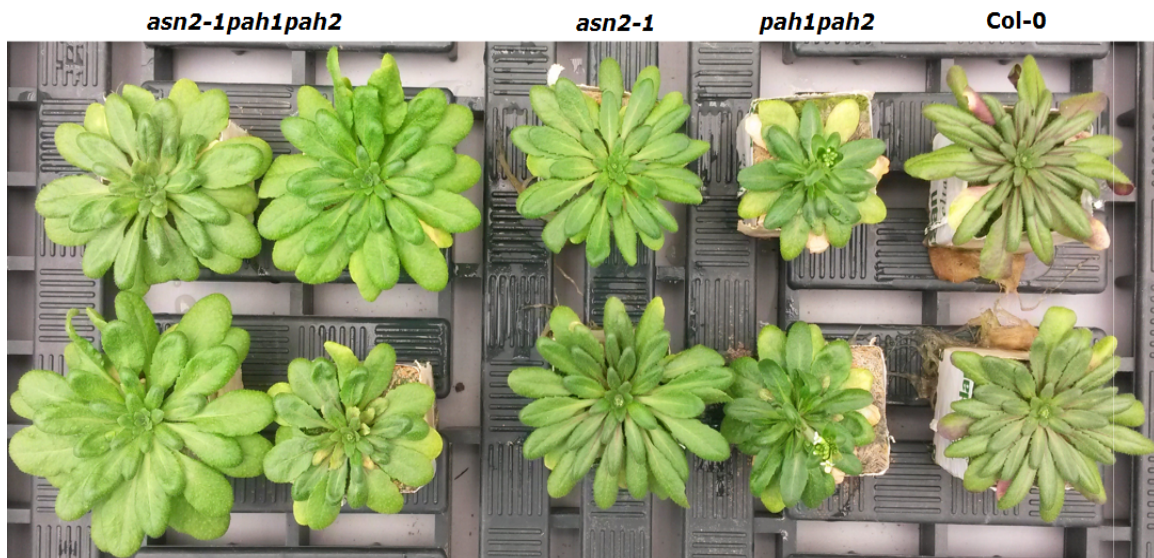


Figure 20: Photograph taken in climate chamber C14 from the four triple mutants, *asn2-1*, *pah1pah2* and Col-0

qRT-PCR

A qRT-PCR experiments were performed to see if the epistatic interaction is expression-related, and to provide insights into the hypothesis that the MGDG and DGDG synthase genes are involved in the photosynthetic phenotype. Therefore, RNA was isolated from three biological replicates per genotype from plants grown under continuous low light ($100 \mu\text{mol photons m}^{-2} \text{s}^{-1}$) and plants 3h after transfer from low to high ($550 \mu\text{mol photons m}^{-2} \text{s}^{-1}$) light. Quantity and quality of RNA was assessed with a Nanodrop2000, with 260/280 ratios between 1.90 and 2.12 and 260/230 ratios between 1.91 and 2.19 with the vast majority with values >2.0 .

Fold changes were calculated based on Cq values. In total three biological samples were removed from analysis; a *pah1pah2* high light sample, a Ts-1 low light sample and a triple mutant high light sample (RNA isolation failed). Based on morphology plants seemed uniform per genotype per light condition except for the triple mutant. Most triple mutants were relatively small and fragile, and many of these had died before the end of the experiment. Death was in most cases due to movement of the black rubber, which pulled the roots out of the rock wool block. In this experiment there was large variation between the two high light triple mutant samples; one sample was relatively very small and showed clear signs of stress (anthocyanin accumulation). In [Error! Reference source not found.](#) the results for the triple mutant are therefore not reliable.

Expression of *ASN2*, *PAH1* and *PAH2*

In **Figure 21** the expression of the studied genes, relative to the housekeeping genes, is plotted. Significant differences in expression between low and high light intensity are depicted with a black asterisk between the two treatments. Also the expression within the same light intensity, between Col-0 and another genotype were compared in **Figure 21**, with significant differences denoted with a red asterisk.

None of the three genes is significantly induced upon high light intensity (**Figure 21 a-c**). In *asn2-1* and the triple mutant no *ASN2* expression was measured under both light intensities as expected (**Figure 21a**). Expression of *PAH1* and *PAH2* was not completely knocked out in the *pah1pah2* and triple mutants (for *PAH1* see **Figure 21b**). The first qRT-PCR of these genes showed expression of both genes under both light intensities. In this first attempt for *PAH1* the primers: PAH1_QF1 and

PAH1_QR1 were used, and for *PAH2*: at5g42870_F and at5g42870_R (**Figure 22** (primer information in **Table S1**: Primer information)). Expression was expected to be completely knocked out for both genes. Therefore, in order to test if the primers were specific, the qRT-PCR was repeated with new primers (PAH1_QF2 and PAH1_QR2; PAH2_QF2 and PAH2_QR2 (**Figure 22**)). No statistical differences were seen between the different sets of primers in all genotypes, except in *pah1pah2* and in the triple mutant. No *PAH2* expression was measured under both light conditions in either *pah1pah2* or the triple mutant with the new set of primers. *PAH1* expression was still measured. Under high light the expression of *PAH1* was significantly lower relative to the housekeeping genes in *pah1pah2* compared to Col-0 under high light ($p=0.001$) (**Figure 21b**). No other significant differences in expression of *ASN2*, *PAH1* and *PAH2* were seen in any of the mutants compared to Col-0 (**Figure 21 a-c**).

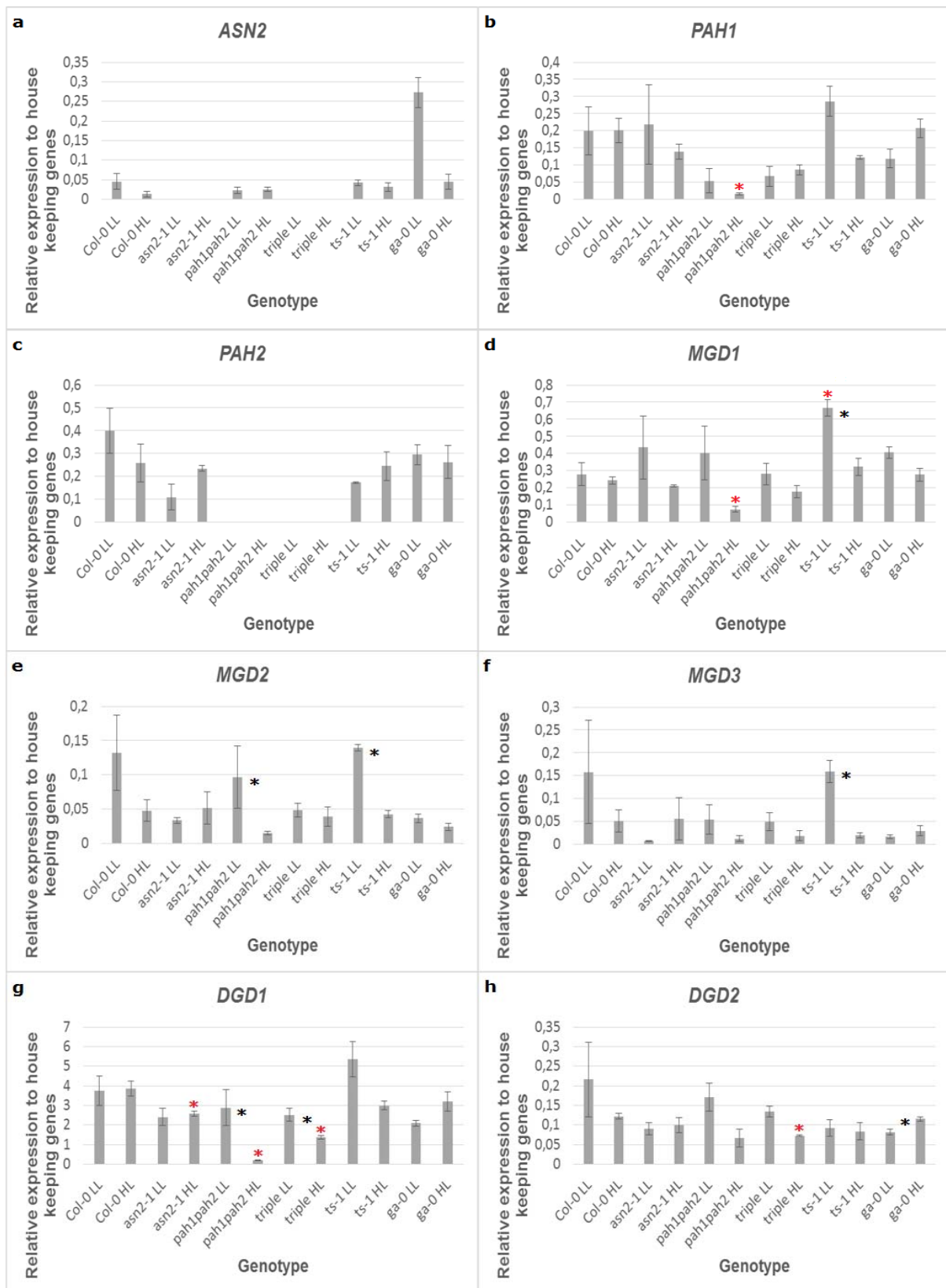


Figure 21: Relative expression to the housekeeping genes *UBQ7* and *CB5E* under low light (LL) intensity and transferred to high light (HL) intensity (100 and 550 $\mu\text{mol photons m}^{-2} \text{s}^{-1}$ respectively). Black asterisk between two bars (*) show a significant difference within the same genotype between low and high light intensity. A red asterisk above a bar (*) show significant differences between Col-0 and another genotype within the same light intensity. Error bars are SE.

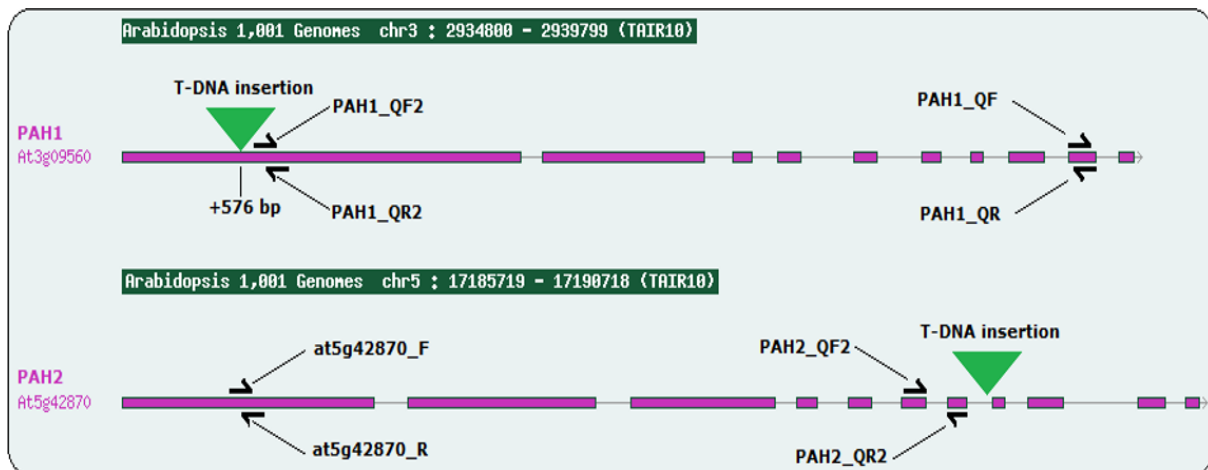


Figure 22: Schematic overview of the exons (purple boxes) of *PAH1* and *PAH2* with annealing positions of the qRT-PCR primers (half black arrows) and the position of T-DNA insertions (green triangles).

Expression of the MGDG and DGDG synthases

A hypothesis for the photosynthetic response to high light of different alleles in *ASN2* and *PAH2* is that these alleles exert their effect via lipid remodelling of chloroplast membranes. Therefore in this study expression of all *Arabidopsis* MGDG (*MGD1*, *MGD2* and *MGD3*) and DGDG synthases (*DGD1* and *DGD2*) were studied (**Figure 21 d-h**). The most changes in expression upon the transfer to high light intensity are seen in Ts-1 with significant downregulation of *MGD1* ($p=0.02$), *MGD2* ($p=0.008$) and *MGD3* ($p=0.01$). In the two other natural accessions, Col-0 and Ga-0, this significant downregulation is not seen. Only in Ga-0, the expression of *DGD2* is significantly upregulated upon transfer to high light ($p=0.04$).

The light experiment was repeated in order to get the data set complete regarding the triple mutant, see **Figure 23**. In the dataset one Col-0 low light sample was removed that showed aberrant expression for all genes. In **Figure 23** for expression of *PAH2* the original set of primers was used (by accident). In the triple mutant, *MGD2* ($p=0.02$), *MGD3* ($p=0.048$) and *DGD2* ($p=0.02$) were significantly upregulated. The significant upregulation of *MGD3* and *DGD1* in Col-0 in **Figure 23** were not seen before in **Figure 21**. The upregulation of *MGD3* in Col-0 is not as extreme as in the triple mutant. Because of this difference between the two experiments, the expression in Col-0 was compared for all genes under both light conditions between the two experiments in order to assess if the separate experiments were comparable. Expression of *ASN2*, *PAH1* and *MGD2*, all under high light intensity differed ($p=0.02$, $p=0.03$ and $p=0.001$ respectively).

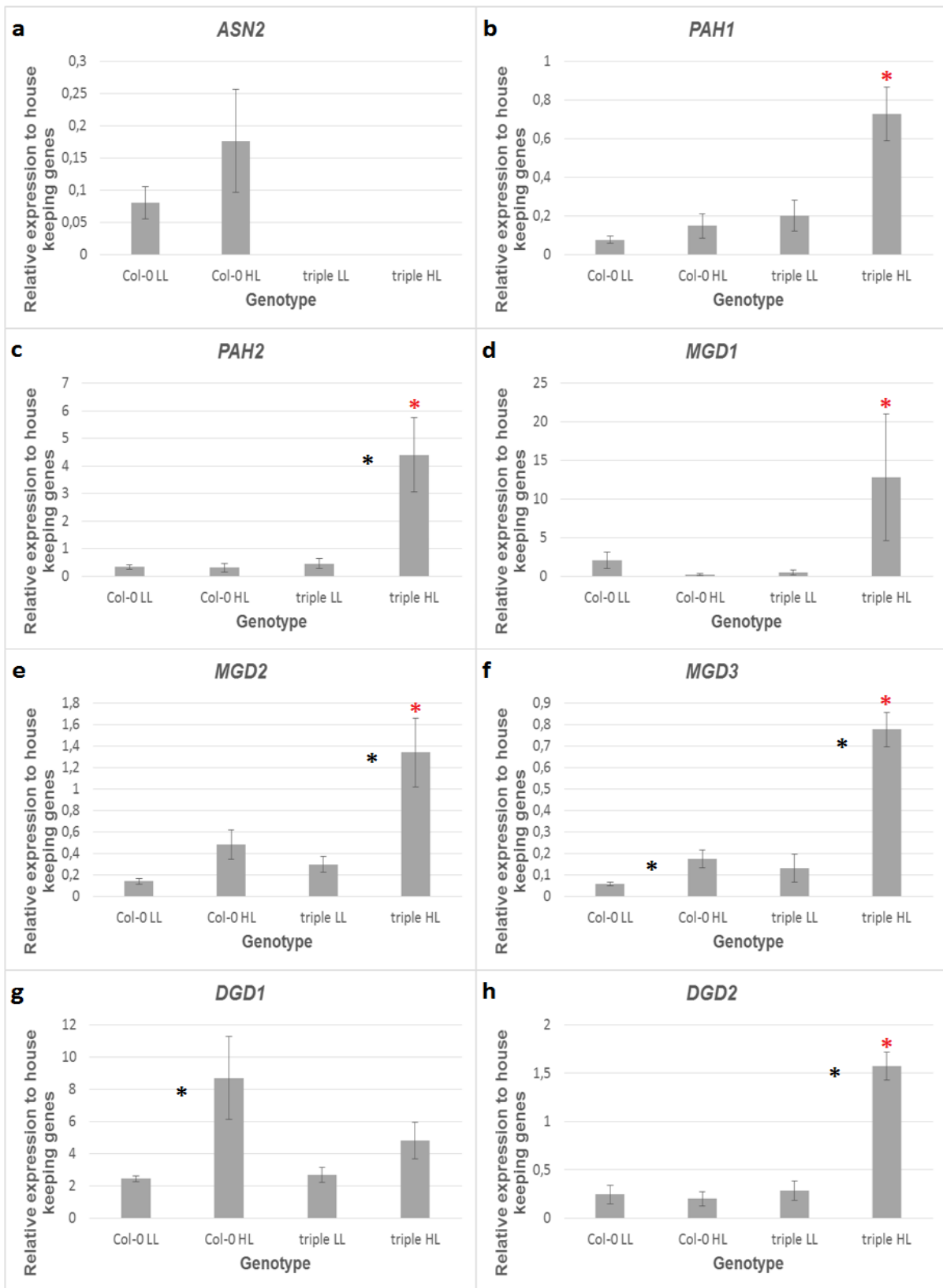


Figure 23: Relative expression in Col-0 and the triple mutant to the housekeeping genes *UBQ7* and *CBSE* under low light intensity and transferred to high light (HL) intensity (100 and 550 $\mu\text{mol photons m}^{-2} \text{s}^{-1}$ respectively). Black asterisk between two bars (*) show a significant difference within the same genotype between low and high light intensity. A red asterisk above a bar (*) show significant differences between Col-0 and another genotype within the same light intensity. Error bars are SE.

Photosynthesis

The photosynthesis efficiency was measured to quantify how the different mutants and wild type accessions perform under different light treatments. The relative electron transport rate (rETR) was calculated for plants growing under continuous light intensities under the four different light intensities (**Figure 24**). No significant differences were observed for any genotype, nor any light intensity. When light response curves were compared between plants grown under continuous light intensity versus plants that were moved from low to high light, only *pah1pah2* ($p=0.05$) differed significantly (**Figure 25**). This figure shows that plants that were moved to $550 \mu\text{mol photons m}^{-2} \text{s}^{-1}$ have adapted to this higher light intensity, since their photosynthesis response is the same as that of plants grown under continuous high light. Finally the photosynthesis response was measured before and after the transfer from low to high light intensity (**Figure 26**). As can be seen in **Figure 26b**, the photosynthesis efficiency is initially relatively high when plants were growing under continuous low light intensity. The day after the transfer to high light intensity the photosynthesis efficiency makes a large drop which slowly recovers in the following days. No significant differences in this response, or the extent of the response were seen between genotypes.

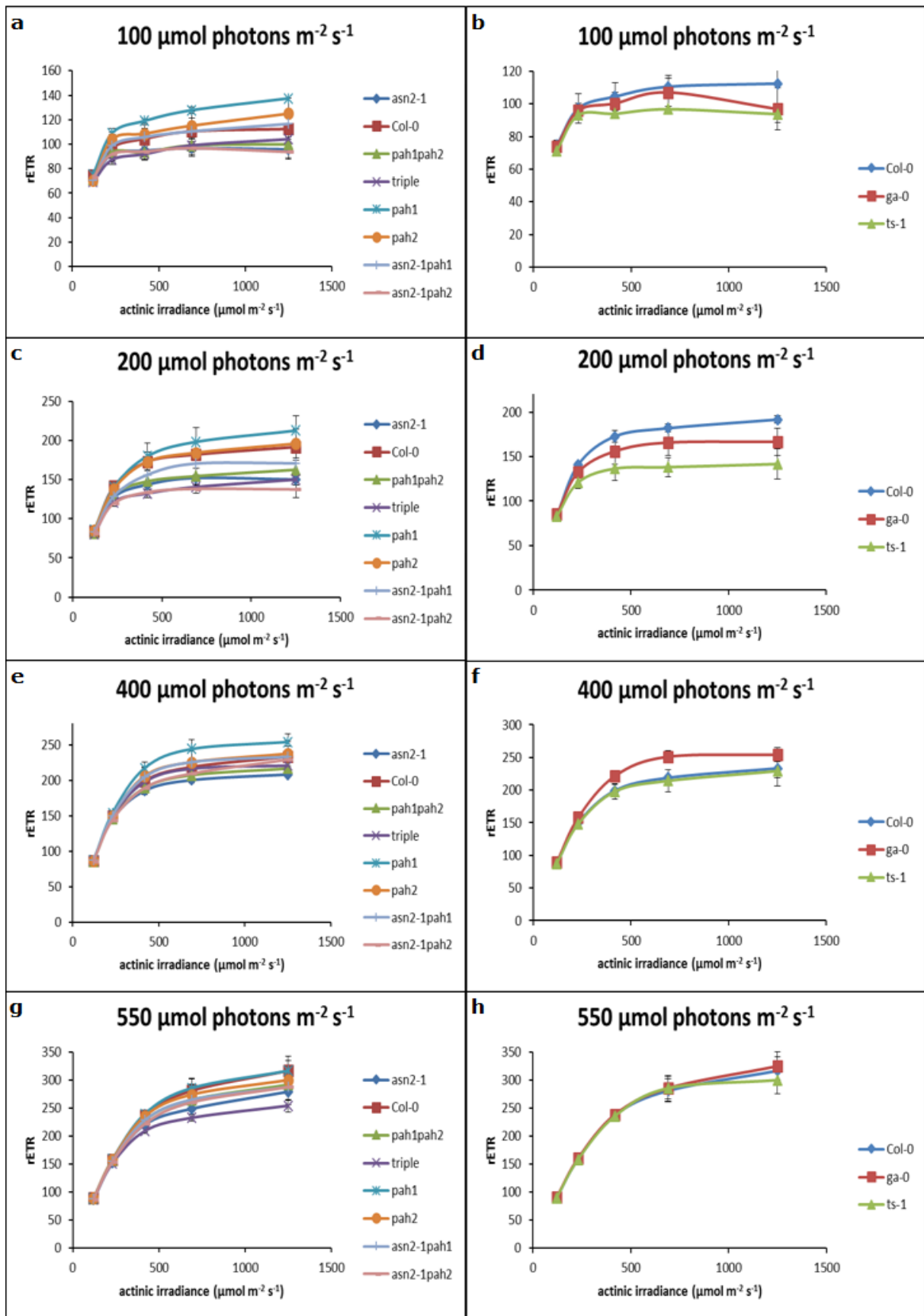


Figure 24: Light response curves from the different genotypes under the four light intensities. rETR is the relative electron transport rate, calculated as: $rETR = \Phi_{PSII} * \text{photon flux density}$. Error bars are SE.

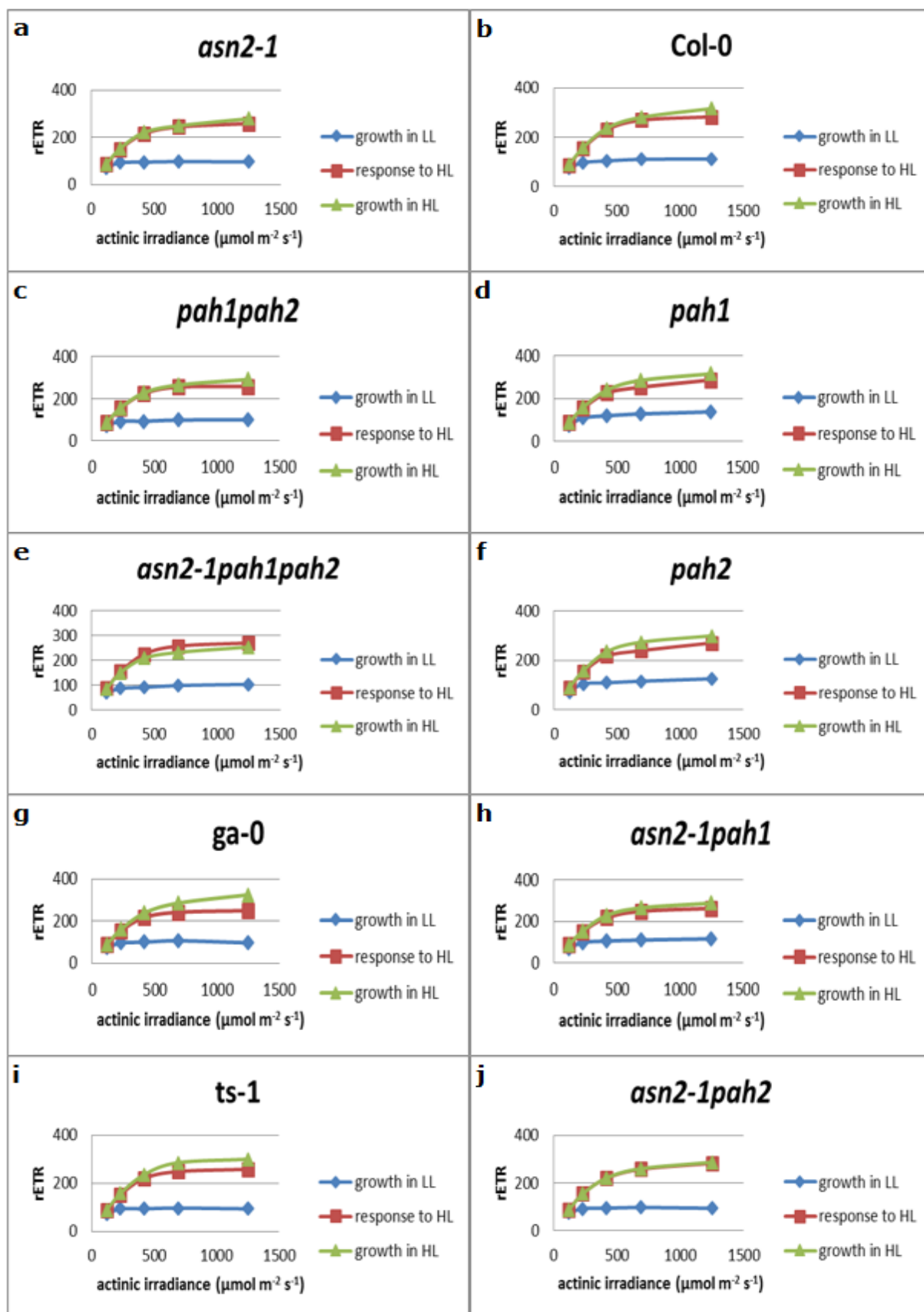


Figure 25: Light response curves from the different genotypes under both continuous light conditions and the plants moved from low to high light intensity (response). rETR is the relative electron transport rate, calculated as: $rETR = \phi_{PSII} \cdot \text{photon flux density}$. Error bars are SE.

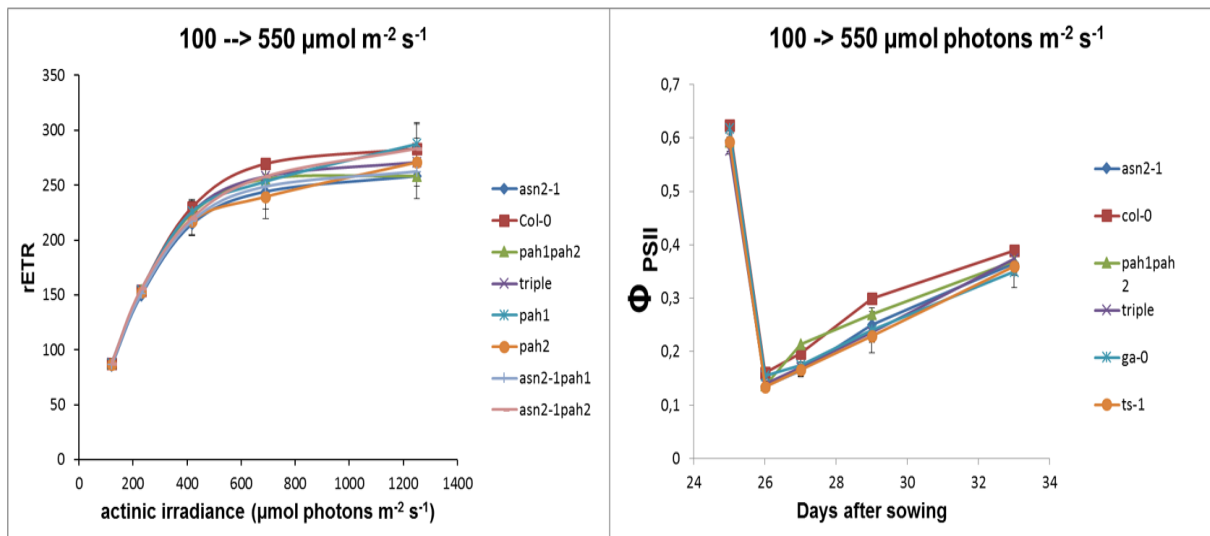


Figure 26: Light response curves for the different genotypes from plants that were moved from 100 to 500 $\mu\text{mol photons m}^{-2} \text{s}^{-1}$. **a)** rETR is the relative electron transport rate, calculated as: $\text{rETR} = \Phi_{\text{PSII}} * \text{photon flux density}$. **b)** Φ_{PSII} of the different genotypes over time from plants that were moved from 100 to 500 $\mu\text{mol photons m}^{-2} \text{s}^{-1}$ after 25 days after sowing. Error bars are SE.

Repetition of photosynthesis measurements

Previous experiments had shown significant differences in photosynthesis efficiency between Ts-1 and Col-0/Ga-0. Therefore, the photosynthesis response from plants transferred from low to high light intensity was repeated, but this time by making use of an automatic phenotyping platform that was also used in previous experiments, see **Figure 27**. The photosynthetic response of the natural accessions Col-0, Ga-0 and Ts-1 was similar in this repetition to the previous experiments, with again Ts-1 having significantly lower photosynthesis efficiency over all time points compared to Col-0. Also *asn2-1* and *pah1pah2* show a similar response as in previous experiments. The triple mutant shows a response that is similar to Col-0, *asn2-1* and *pah1pah2*.

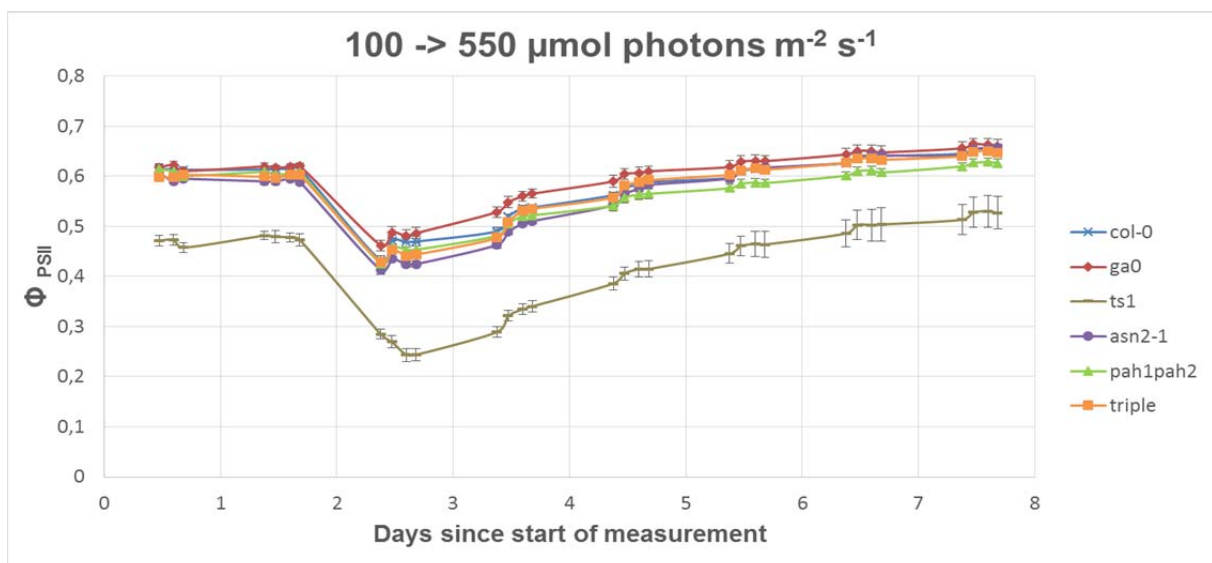


Figure 27: Φ_{PSII} of the different genotypes over time from plants that were moved from 100 to 550 $\mu\text{mol photons m}^{-2} \text{s}^{-1}$ after light offset on day 2 of the measurement. Error bars are SE.

The photosynthesis response of Col-0, *asn2-1*, *pah1pah2* and the triple mutant seem to be quite similar to each other, however when this response is examined into more detail there are differences in the photosynthesis response between the different mutants. In **Figure 28a** the photosynthesis efficiency response of Col-0, *asn2-1*, *pah1pah2* and the triple mutants are shown again, but zoomed in. The *pah1pah2* double mutant is under low light intensity, and the first days similar to Col-0, but starts to deviate from Col-0 under high light conditions over time. In **Figure 28b** the photosynthesis response of the different mutants are compared to Col-0 with a two-sided t-test for each time point, and shows this *p*-value. *pah1pah2* has similar photosynthesis efficiency under low light intensity, but this slowly starts to decrease and deviates from Col-0. Around day 5 of the measurement (3 days of high light intensity) this difference in photosynthesis efficiency becomes significant. *asn2-1* on the other hand has significantly lower photosynthesis efficiency during most of the time points under low light intensity and the first two days after high light intensity. The triple mutants seems to resemble the response seen in *asn2-1* most.

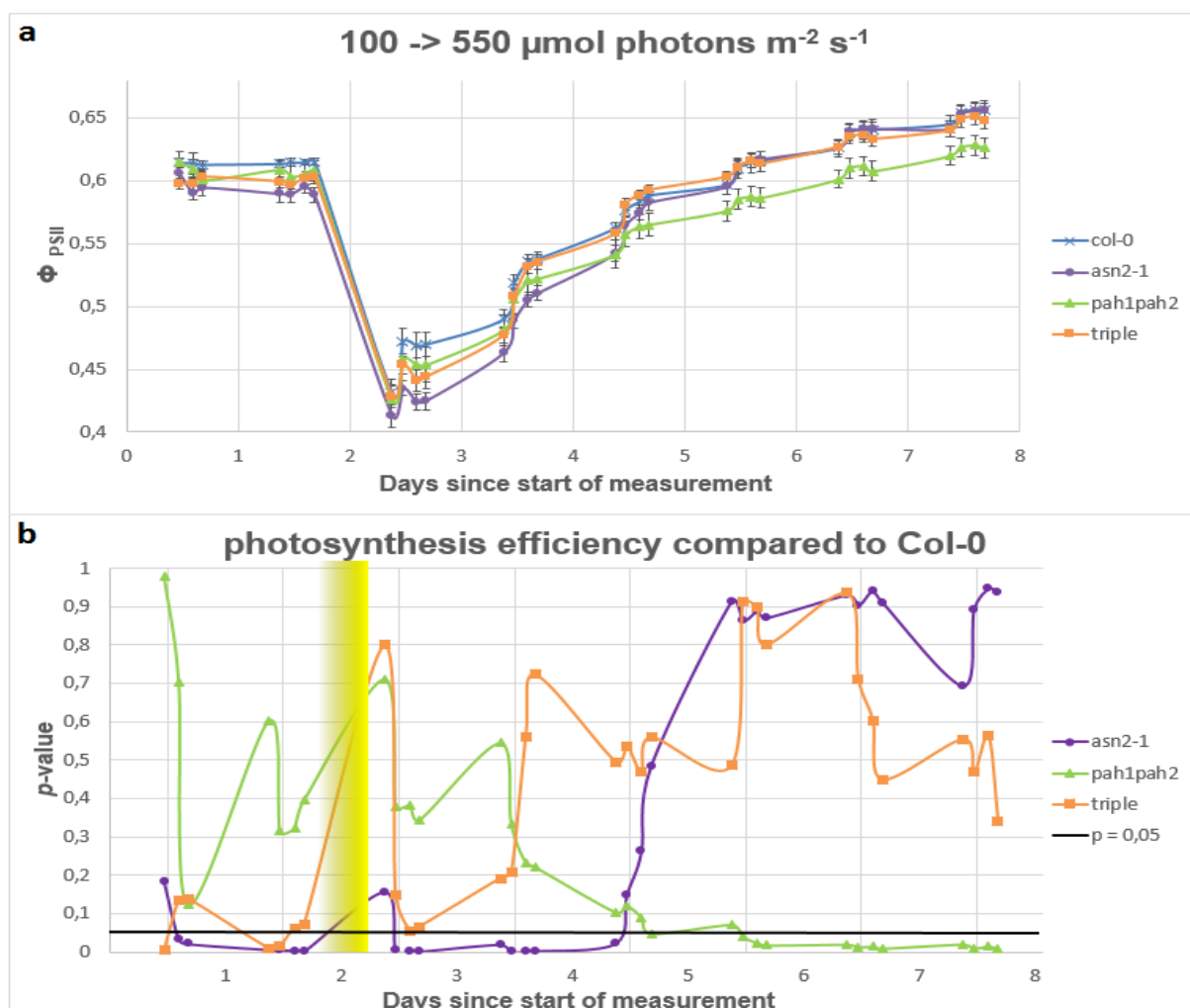


Figure 28: a) Φ_{PSII} response over time, same as **Figure 27** but zoomed in and without the accessions Ga-0 and Ts-1. b) Φ_{PSII} of the different mutants compared to Col-0 at each time point (two sided t-test). Points under the black line ($p = 0.05$) are considered significantly different. The yellow bar represents the switch from low to high light intensity.

Discussion

Molecular cloning

Molecular cloning of these two relatively large insert sizes by Gateway technology has proven to be challenging, with only one positive clone found for *ASN2* and no successful transformants at all for *PAH2*. Efficiency of the Gateway cloning is affected by numerous aspects, of which the insert size and the final plasmid size are important (**Petersen and Stowers 2011**). A study in which around 12000 *Caenorhabditis elegans* ORFs were cloned by Gateway technology showed that cloning efficiency was inversely proportional to the insert size (**Reboul et al. 2003**). Although both fragments were quite large, both should be theoretically possible to clone with the Gateway cloning technique. This is especially the case of *ASN2* since the total insert size was 4193 bp, which is a size that is generally not considered to be too large for efficient cloning.

For the *PAH2* insert (6851 bp) the size is becoming more of a problem. **Petersen and Stowers (2011)** for example cloned many different insert sizes up to a maximum of about 6kb in size, however failed in multiple attempts to clone inserts ranging from 7 to 11 kb. Because of the lower efficiencies due to increased size, other factors (competence of cells, quality of DNA etc.) should be optimal to obtain correct clones. The results from *ASN2* show therefore that most likely not all other factors were optimal. This is most likely due to a combination of multiple reasons; own prepared competent cells do not have equally high competence to commercial cells, the concentration of DNA that was added was measured by a Nanodrop 2000 which does not always give accurate amounts. Furthermore the amount of DNA that is provided to the electroporation reaction can also influence the efficiency of transformation and the number of colonies. In this study 1 μ L (30 ng) from the BP reaction was used, as was recommended in the protocol, but this might not be the optimal amount. Another factor that might have impeded efficient cloning of *PAH2* is the possible presence of strong secondary structures in the DNA. Except for a double helix, DNA can fold into different inter- and intrasecondary structures (**Bochman et al. 2012**). These secondary structures may impede efficient cloning of such fragments. Amplification of the fragment was already difficult with multiple primer sets (**Figure 8b+c, Figure 9**) which might be caused by formation of secondary structures. Such structures are mostly known to form in GC rich areas (**Bochman et al. 2012**). Both the promoter and terminator region of the *PAH2* locus do not have a high GC content (35 and 33% respectively), and known secondary structure forming motifs such as G-quadruplex structures are also not present.

Gibson Assembly seems to be a good alternative for cloning of large inserts. The method is easy to apply and fast. The ratio of correct clones was still quite low (8/46 colonies that were tested). Therefore, in future attempts with Gibson Assembly it would be recommended to decrease the total number of fragments (this increases cloning efficiency), or divide the vector backbone into two parts which both contain half of the antibiotic resistance gene to decrease the number of false positives, however this last suggestion then again leads to increased number of fragments.

The first objective of this project was to clone both the high and low alleles from *ASN2* and *PAH2*. In order to complete this, several strategies could be used. For both genes the same strategy could be applied, however some improvements should be considered. DNA purification by gel extraction for cloning of *ASN2* would be a better alternative than DNA purification by a standard kit since it should completely circumvent colonies harbouring empty vectors that are created by recombination with primer dimers. Furthermore, the aim of this study is only to create one correct expression clone per

allele. The entry clone is solely used as an intermediate step to obtain the expression clone. Therefore, the BP and LR reaction could be combined into a single reaction (Liang et al. 2013). This strategy would circumvent one electroporation, miniprep and restriction enzyme digestion pattern to screen for correct entry clones. However given the low rate of success for *ASN2* by Gateway cloning, also other options should be considered such as Gibson Assembly. The PCR of *ASN2* with the Gateway primer gave very good results for some samples, therefore designing Gibson Assembly suitable primers that amplify the whole *ASN2* allele as a single fragment can be recommended to keep the total number of fragments as low as possible (only two). To obtain the other *PAH2* allele, it seems to be the fastest to repeat everything, the method provides within rather limited time an expression clone. A cheaper, yet similar approach to Gibson Assembly is Seamless Ligation Cloning Extract (SLiCE) cloning. SLiCE cloning uses bacterial cell extracts to assemble DNA fragments into recombinant DNA molecules in a single reaction (Zhang et al. 2012). The technique only relies on cell extracts from *E. coli* RecA⁻ strains such as TOP10 or DH10B) and commonly used buffers (Zhang et al 2012). Similar to Gibson Assembly, SLiCE makes use of recombination between short regions of homology between fragments. Also, expression clones with the different alleles might be created by using the Q5 Site-Directed Mutagenesis Kit (NEB) that is designed to create site-specific SNPs into vectors.

Generation of the triple mutant *asn2-1pah1pah2*

The phenotype of the *asn2-1pah1pah2* triple mutant resembled the *asn2-1* and is quite easily recognisable. Both **Error! Reference source not found.** and **Error! Reference source not found.** showed that the triple mutant remained the smallest, independent of the light intensity. The delayed growth therefore also caused many triple mutants to die before the end of the experiment. Interestingly, a picture taken in a different growth chamber (C14) than the four triple mutants that were found, showed a quite different response (Figure 20). Three out of four triple mutants are larger than the other genotypes, including Col-0, which was always among the largest/heaviest in the light experiment. In C14 a tide system was used to supply the plants from water and nutrients, while in D2 plastic trays were used in which the nutrient solution was poured. The temperature and day length were the same among the two growing conditions. A possible explanation for the differences in this triple mutant might be that the first generation of the triple mutants (C14 plants) was obtained by selfing heterozygous plants for the T-DNA insertion and wild type allele of *ASN2*, while the second generation of triple mutants (D2 plants) was obtained as offspring from a homozygous T-DNA insertion mutant. Nam et al. 2003 saw enhanced nitrogen status in seeds from *ASN1* overexpressing lines. The seeds from these overexpressing lines also contained elevated soluble seed proteins. If the opposite would also be true, that a homozygous knockout would lead to a reduced nitrogen status in the seeds, this might (partially) explain the difference between the two generations of triple mutants. The first generation of triple mutants was the result of selfing an *ASN2asn1pah1PAH2pah2* plant, and therefore a functional copy of *ASN2* was still present. A triple mutant has difficulties in its nitrogen and phosphate homeostasis, and therefore the seeds of this triple mutant might have reduced levels of these nutrients. This does however not explain why the first generation of triple mutants was larger than Col-0 plants in C14.

Light experiment

The different light treatments

In the light experiment five different light treatments were used, four treatments with continuous light ranging from 100 to 550 $\mu\text{mol photons m}^{-2} \text{s}^{-1}$ and one treatment with plants that moved from 100 to 550 $\mu\text{mol photons m}^{-2} \text{s}^{-1}$. The two extreme light conditions were most important, as they were also used in earlier experiments that detected these candidate genes, while the two intermediate intensities were created with the idea that certain genotypes possibly would do relatively very well under either low or high light intensity, but relatively bad under a contrasting light intensity. The two intermediate light intensities could then have shown this response in a more gradual manner. This was however not the case, and therefore in future experiments these two intermediate light intensities might be removed from the experiment.

RT-qPCR

ASN2, PAH1 and PAH2

From the three tested genes, only *ASN2* expression is known to be affected by light. The results that are shown here indicate that *PAH1* and *PAH2* are not directly regulated by light. Under 'normal' growing conditions (150 $\mu\text{mol photons m}^{-2} \text{s}^{-1}$) *ASN2* expression follows a diurnal pattern in which expression is high in the dark, and low in the light (**Gaufichon et al. 2013**). Expression can be induced by high light irradiation, however this is ammonium dependent (**Wong et al. 2004**). When *ASN2* expression was measured in plants grown under continuous high light, it showed after 4 hours the first induction of expression on a Northern-blot (**Wong et al. 2004**). Under salt and cold stress *ASN2* was significantly upregulated after eight and 16 hours but not after two and four hours because ammonium levels had to build up (**Wong et al. 2004**). In this study expression of *ASN2* was not affected by the increase in light intensity, possibly because not enough ammonium had been built up in these 3 hours for upregulation of *ASN2*. Therefore a time-course experiment in which RNA is sampled during multiple times during the first day of high light (and in low light as a control) can be interesting. Perhaps inducing of *ASN2* might also be followed by induction of *PAH2*.

PAH1 and *PAH2* were expected to have no expression in *pah1pah2* (**Eastmond et al. 2010**) but this was not the case. *PAH1* was still expressed with both sets of primers, while for *PAH2* the position of the primers made the difference between the absence or presence of measuring expression. Therefore, for *PAH2* it is likely that a truncated protein is being formed.

In order to better understand the unexpected results seen in *pah1pah2*, the qRT-PCR primers from (**Eastmond et al. 2010**) were examined. Alignment of the primers showed that a region of 899 and 833 bp was amplified for *PAH1* and *PAH2* respectively, and that the primers were situated up- and downstream of the T-DNA insertion and thereby increasing the amplicon length in *pah1pah2*, see **Figure 29**. Amplicon length in qRT-PCR should not exceed 150 bp (**Udvardi et al. 2008**) which might explain why the authors did not find any expression. Furthermore in a micro array study by the same group, a significant upregulation of *PAH2* was found compared to Col-0 in *pah1pah2* (**Craddock et al. 2015**). The mRNA that is produced will most likely not be functional. The NCBI conserved domain tool (<http://www.ncbi.nlm.nih.gov/Structure/cdd/wrpsb.cgi>) predicts a function domain in *PAH2* that ranges almost the end of intron #3 until the very end of intron #8 on **Error! Reference source not found**.. The second pair of primers, which did not show expression of *PAH2*, lay in the middle of this important domain, thus the protein is most likely not (fully) functional.

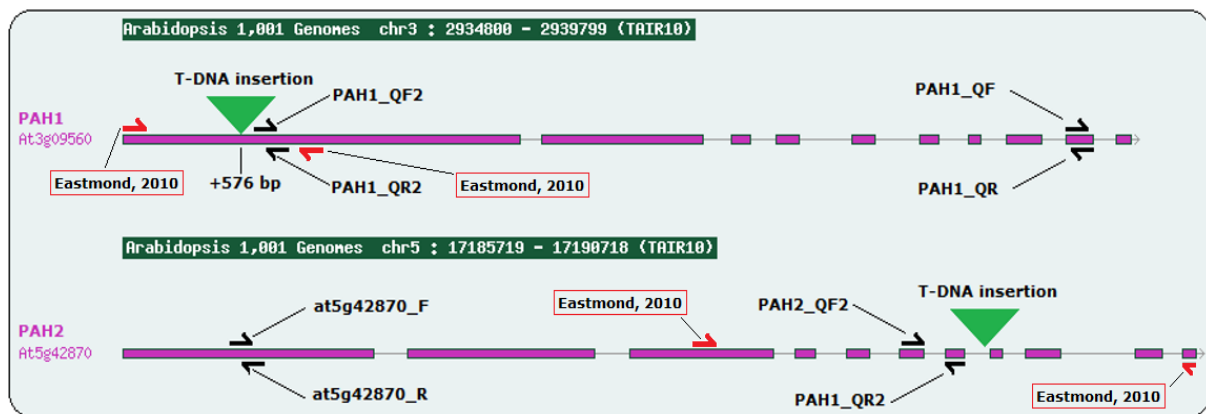


Figure 29: Schematic overview of the exons (purple boxes) of *PAH1* and *PAH2* with annealing positions of the qRT-PCR primers (half black arrows) and the position of T-DNA insertions (green triangle). Half red arrows are the primers used by **Eastmond et al. 2010**.

MGDG and DGDG synthases

Alterations in expression upon high light of the different MGDG and DGDG synthase genes compared to Col-0 were mainly seen in *Ts-1*, *pah1pah2* and the triple mutant. Interestingly the triple mutant shows almost an opposite expression pattern compared to *pah1pah2* (i.e. upregulation of several genes in the triple mutant, and downregulation in *pah1pah2*). The differences between this double and triple mutant are large and might be partially caused by the difference in the experimental setup (expression of *MGD3* and *DGD1* were also significantly upregulated in the second experiment in Col-0, but not in the first). In the repetition of the light experiment the tide system was used for watering of the plants and light intensities were created in the whole climate chamber by adjusting the light source, rather than shading with cloth. Overall this might have caused differences in temperature, light intensity and/or quality and overall homogeneity of different samples. Nevertheless, expression of the eight genes in Col-0 was similar among the two experiments in the most cases.

The qRT-PCR results show in several cases high standard deviations. At least three biological replicates should be used (**Udvardi et al. 2008**) in qRT-PCR, which could not always be fulfilled in this study for all genotypes under both light intensities. In most cases the large standard deviation was caused by one sample that deviated to a large extent while the other two samples were similar. For *PAH1* and *PAH2* the qRT-PCR was repeated with different primers, and these repetitions showed that the samples were different. Furthermore, the SD between technical replicates was low, and thus these differences are no measurement errors. In future studies it would be recommended to increase the number of biological replicates. By using eight plants per genotype, and pooling two plants into four biological replicates, the effects of single outlying samples should decrease to a large extent.

Another possible important factor that should be taken into consideration is the fact that the genotypes studied here showed differences in growth under all light conditions (**Figure 18, Figure 19**). Therefore the studied samples are not in the same developmental stages, which might cause differences in expression.

In the first light experiment the different light intensities were created by shading with different kinds of cloths. This approach is not optimal since more factors can be affected aside from only light intensity. Temperature definitely differed between light compartments, with higher temperatures at

higher light intensities. These temperature differences were partially created by the shading with cloth, and in case of the highest light intensity also partially by the distance to the light source; plants at the highest light intensity were put on a plateau on the table and were closer to the light source. Differences in temperature have not been measured, but were noticeable by sense. Other factors that might have been different among treatments are humidity and light spectrum which might have been differentially affected by the different cloths that were used. Although higher temperatures will co-occur with higher light intensities (full sun) in nature, in future experiments the temperature should be more stable among different light treatments. Temperature is known to affect the relative amount of galactolipids and the DGDG to MGDG ratio (Chen et al. 2006).

Photosynthesis

The first photosynthesis results showed no significant differences in photosynthesis efficiency between any of the genotypes under any light intensity. There were some differences between this and the previous experiments which (might) explain this differences in the photosynthesis response. The climate chamber was divided into four compartments with different light intensities in the current experiment, while in the previous experiment only one light intensity was created in the whole climate chamber. These different compartments might have differences in homogeneity of the light intensity. Another difference is that in this experiment the hydroponic solution was poured in plastic containers that were holding the rock wool blocks with the plants, while in the previous experiment a tide system was used to provide the plants with the hydroponic solution. Furthermore, the edges of the plastic containers that were holding the plants, were leaning on the round PVC construction that were used to create the surroundings of the different light compartments. Thereby, the edges of the plastic containers were slightly elevated, which caused the hydroponic solution to congregate in the centre of the plastic container, which might also have caused differences in homogeneity. It was checked on regular bases if the outside rock wool blocks were not too dry, but this was never the case. However the opposite might be true, that rock wool blocks in the centre were too wet. Finally, and most likely the most important, another camera was used for the chlorophyll fluorescence measurements. In this experiments plants were moved from the climate chamber to the camera which most likely has caused stress. In the previous experiment the automatic phenotyping platform was used for these measurements.

When later this experiment was repeated with the automatic phenotyping platform, the photosynthesis efficiency results were similar to previous experiments. *pah1pah2* had reduced photosynthesis efficiency under high light conditions, while *asn2-1* seemed mainly affected under low light intensity. The triple mutant showed an intermediate response that mostly resembled *asn2-1*. A possible explanation is that, as mentioned before, *pah1pah2* is known to have altered lipid compositions which affects membrane stability and thereby photosynthesis efficiency. Under stress conditions plants adapt their membrane compositions in order to be better able to cope with stress. The low light intensity will not cause as much stress (i.e. ROS or ammonium), which allows *pah1pah2* to have normal photosynthesis. However, under high light conditions *pah1pah2* is not, or far less, able to adapt its membranes. This leads to reduced photosynthesis efficiency caused by the increase of stress due to the higher light intensity.

asn2-1 was most affected in its photosynthesis under low light intensity, which is unexpected since *ASN2* is known to function under the combination of high light and ammonium. More ammonium will be present under high light irradiance and therefore my hypothesis was that *ASN2* would mainly

function under these conditions. These results therefore suggest a role for *ASN2* in the photosynthesis response to high light different from ammonium detoxification.

Based on the phenotype (pale green) it seems likely that also the triple mutant has a decreased nitrogen status and decreased amount of chlorophyll, similar to what is known about *asn2-1*. As mentioned before, a decreased nitrogen status can lead to an increase of expression of several of the MGDG and DGDG synthases. The response of the different MGDG and DGDG synthases is however very different from *pah1pah2*, and several genes were indeed upregulated (this was not seen in *asn2-1* however). Therefore, this decreased nitrogen status possibly affected the lipid composition in a positive, more stable, manner that maintains an optimal efficiency. During the same light experiment from each genotype also three biological replicates were harvested for a lipid assay. These results will further explore this hypothesis.

Nevertheless, the studied response to high light was about the epistatic interaction between *ASN2* and *PAH2*. The triple mutant was the least affected from the different mutants in terms of photosynthesis. As compared to the natural alleles, an epistatic interaction can also be observed between the different knockout mutants, both in the qRT-PCR and in the photosynthesis efficiency experiments. In the qRT-PCR experiment, for example, expression of *DGD2* is not altered upon high light induction in either *asn2* or *pah1pah2* (**Figure 21h**). However, in the triple mutant *DGD2* expression is significantly upregulated (**Figure 23h**). Although there might be differences between the two experiments, the response of Col-0 is similar among both experiments. The epistatic interaction can also be observed in the photosynthesis experiment. *asn2* shows significant differences in photosynthesis efficiency compared to Col-0 for the first few days of the measurements, while *pah1pah2* starts to differ from Col-0 after two days of recovering from the high light stress. Both genes, when knocked out, have a negative effect on photosynthesis efficiency during some part of the experiment (since photosynthesis efficiency is significantly lower for the mutants during some part of the experiment). My hypothesis was that if you increase the number of knocked out genes that negatively affect photosynthesis, that this would further decrease overall photosynthesis efficiency, or that that the effects of single knockouts would be additive in the triple mutant. This would mean that the triple mutant would have lower photosynthesis efficiency at low light intensity and during the first two days of recovery due to the *asn2* effect, and then take over the slow recovery from *pah1pah2*. However, the triple mutant shows at only three time points significant differences compared to Col-0, whereas *asn2* differs at 14 time points and *pah1pah2* at 12 time points. The triple mutant is in its overall photosynthesis less affected than either *asn2-1* and *pah1pah2*.

Overall, the first objective, to clone the low and high alleles from *ASN2* and *PAH2* has not been finished. The cloned alleles have thus also not been transformed into the triple knock out mutant *asn2-1pah1pah2* that has been successfully obtained (objective 2). The purpose of this cloning approach was to do an allelic complementation test that could prove the epistatic interaction between the two genes under study. The allelic complementation test has not been performed and therefore this final proof has not been delivered, however the qRT-PCR and photosynthesis experiments on the different wild type accessions and mutants have provided further evidence of an epistatic interaction. The photosynthesis measurements have falsified my hypothesis that photosynthesis efficiency would be more affected in the triple mutant compared to either *asn2-1* or *pah1pah2*. The triple mutants were affected in their growth (based on size and weight), however this

is most likely due to an partial inability to regulate nitrogen and/or phosphate homeostasis. The results indicate that some MGDG and DGDG are altered in both Ts-1 compared to Col-0 and Ga-0, while also the triple mutant shows distinct different expression compared to *asn2-1* and *pah1pah2*. If these changes are a direct effect of the epistatic interaction between *ASN2* and *pah1pah2* or an indirect effect caused by phosphate, remains unclear. This study therefore has provided more evidence of the epistatic interaction between *ASN2* and *PAH2*, and has provided more insights into the processes that are affected by these genes.

Acknowledgements

The author would like to thank Mark Aarts for useful comments and remarks, and for accepting me into the group. Furthermore I would like to thank Roxanne van Rooijen for introducing me into this subject, teaching me several new techniques and the daily supervision. Also the suggestions given by Robert Akkers, Tânia Serra and Valeria Ochoa regarding the molecular cloning are appreciated.

References

- BAILEY S, WALTERS RG, JANSSON S AND HORTON P. 2001. Acclimation of *Arabidopsis thaliana* to the light environment: the existence of separate low light and high light responses. *Planta* 213: 794-801.
- BENNING C AND OHTA H. 2005. Three enzyme systems for galactoglycerolipid biosynthesis are coordinately regulated in plants. *Journal of biological chemistry* 280: 2397-2400.
- BLOCK MA, DORNE A-J, JOYARD J AND DOUCE R. 1983. Preparation and characterization of membrane fractions enriched in outer and inner envelope membranes from spinach chloroplasts. II. Biochemical characterization. *Journal of biological chemistry* 258: 13281-13286.
- BOCHMAN, ML, PAESCHKE K AND ZAKIAN VA. 2012. DNA secondary structures: stability and function of G-quadruplex structures. *Nature review genetics* 13: 770-780.
- CHEN J, BURKE JJ, XIN Z, XU C AND VELTEN J. 2006. Characterization of the *Arabidopsis* thermosensitive mutant *atts02* reveals an important role for galactolipids in thermotolerance. *Plant, cell & environment* 29: 1437-1448.
- CRADDOCK CP, ADAMS N, BRYANT FM, KURUP S AND EASTMOND PJ. 2015. PHOSPHATIDIC ACID PHOSPHOHYDROLASE regulates phosphatidylcholine biosynthesis in *Arabidopsis* by phosphatidic acid-mediated activation of CTP: PHOSPHOCHOLINE CYTIDYLYLTRANSFERASE activity. *The plant cell* 27: 1251-1264.
- DEMMIG-ADAMS B AND ADAMS III W. 1992. Photoprotection and other responses of plants to high light stress. *Annual review of plant biology* 43: 599-626.
- DEMMIG-ADAMS B AND ADAMS WW. 2006. Photoprotection in an ecological context: the remarkable complexity of thermal energy dissipation. *New phytologist* 172: 11-21.
- EASTMOND PJ, QUETTIER A-L, KROON JT, CRADDOCK C, ADAMS N AND SLABAS AR. 2010. PHOSPHATIDIC ACID PHOSPHOHYDROLASE1 and 2 regulate phospholipid synthesis at the endoplasmic reticulum in *Arabidopsis*. *The plant cell* 22: 2796-2811.

- EVANS JR. 1989. Photosynthesis and nitrogen relationships in leaves of C₃ plants. *Oecologia* 78: 9-19.
- FLOOD PJ, HARBINSON J AND AARTS MGM. 2011. Natural genetic variation in plant photosynthesis. *Trends in plant science* 16: 327-335.
- GAUDE N, BRÉHÉLIN C, TISCHENDORF G, KESSLER F AND DÖRMANN P. 2007. Nitrogen deficiency in *Arabidopsis* affects galactolipid composition and gene expression and results in accumulation of fatty acid phytyl esters. *The plant journal* 49: 729-739.
- GAUFICHON L, MASCLAUX-DAUBRESSE C, TCHERKEZ G, REISDORF-CREN M, SAKAKIBARA Y, HASE T, CLEMENT G, AVICE JC, GRANDJEAN O AND MARMAGNE A. 2013. *Arabidopsis thaliana* ASN2 encoding asparagine synthetase is involved in the control of nitrogen assimilation and export during vegetative growth. *Plant, cell & environment* 36: 328-342.
- HAN, G-S, WU W-I AND CARMAN GM. 2006. The *Saccharomyces cerevisiae* lipin homolog is a Mg²⁺-dependent phosphatidate phosphatase enzyme. *Journal of biological chemistry* 281: 9210-9218.
- HUBER TA AND STREETER JG. 1984. Asparagine biosynthesis in soybean nodules. *Plant physiology* 74: 605-610.
- JUNG H-S, CRISP PA, ESTAVILLO GM, COLE B, HONG F, MOCKLER TC, POGSON BJ AND CHORY J. 2013. Subset of heat-shock transcription factors required for the early response of *Arabidopsis* to excess light. *PNAS* 110: 14474-14479.
- KAGAWA T, SAKAI T, SUETSUGU N, OIKAWA K, ISHIGURO S, KATO T, TABATA S, OKADA K AND WADA M. 2001. *Arabidopsis* NPL1: a phototropin homolog controlling the chloroplast high-light avoidance response. *Science* 291: 2138-2141.
- KARPINSKI S, ESCOBAR C, KARPINSKA B, CREISSEN G AND MULLINEAUX PM. 1997. Photosynthetic electron transport regulates the expression of cytosolic ascorbate peroxidase genes in *Arabidopsis* during excess light stress. *The plant cell* 9: 627-640.
- KELLY AA AND DÖRMANN P. 2002. DGD2, an *Arabidopsis* gene encoding a UDP-galactose-dependent digalactosyldiacylglycerol synthase is expressed during growth under phosphate-limiting conditions. *Journal of biological chemistry* 277: 1166-1173.
- KOBAYASHI K, KONDO M, FUKUDA H, NISHIMURA M AND OHTA H. 2007. Galactolipid synthesis in chloroplast inner envelope is essential for proper thylakoid biogenesis, photosynthesis, and embryogenesis. *Proceedings of the national academy of sciences* 104: 17216-17221.
- LAM HM, HSIEH MH AND CORUZZI G. 1998. Reciprocal regulation of distinct asparagine synthetase genes by light and metabolites in *Arabidopsis thaliana*. *The plant journal* 16: 345-353.
- LARSEN TM, BOEHLEIN SK, SCHUSTER SM, RICHARDS NG, THODEN JB, HOLDEN HM AND RAYMENT I. 1999. Three-dimensional structure of *Escherichia coli* asparagine synthetase B: a short journey from substrate to product. *Biochemistry* 38: 16146-16157.
- LI X, MOELLERING ER, LIU B, JOHNNY C, FEDEWA M, SEARS BB, KUO M-H AND BENNING C. 2012. A galactoglycerolipid lipase is required for triacylglycerol accumulation and survival following nitrogen deprivation in *Chlamydomonas reinhardtii*. *The plant cell* 24: 4670-4686.

- LIANG X, PENG L, BAEK C-H AND KATZEN F. 2013. Single step BP/LR combined Gateway reactions. *Biotechniques* 55: 265-268.
- MAXWELL K AND JOHNSON GN. 2000. Chlorophyll fluorescence—a practical guide. *Journal of experimental botany* 51: 659-668.
- MÜLLER P, LI X-P AND NIYOGI KK. 2001. Non-photochemical quenching. A response to excess light energy. *Plant physiology* 125: 1558-1566.
- NAKAMURA Y, KOIZUMI R, SHUI G, SHIMOJIMA M, WENK MR, ITO T AND OHTA H. 2009. Arabidopsis lipins mediate eukaryotic pathway of lipid metabolism and cope critically with phosphate starvation. *Proceedings of the national academy of sciences* 106: 20978-20983.
- NAKAMURA Y AND OHTA H 2010. Phosphatidic acid phosphatases in seed plants. *Lipid signaling in plants*: Springer, p. 131-141.
- PETERSEN LK AND STOWERS RS. 2011. A Gateway multisite recombination cloning toolkit. *PLoS ONE* 6: e24531.
- REBOUL J, VAGLIO P, RUAL J-F, LAMESCH P, MARTINEZ M, ARMSTRONG CM, LI S, JACOTOT L, BERTIN N AND MOORE T. 2003. *C. elegans* ORFeome version 1.1: experimental verification of the genome annotation and resource for proteome-scale protein expression. *Nature genetics* 34: 35-41.
- SIECIECHOWICZ KA, IRELAND RJ AND JOY KW. 1988. Diurnal changes in asparaginase activity in pea leaves. *Journal of experimental botany* 39: 707-721.
- UDVARDI MK, CZECHOWSKI T AND SCHEIBLE W-R. 2008. Eleven golden rules of quantitative RT-PCR. *The plant cell online* 20: 1736-1737.
- VAN ROOIJEN, R, HARBINSON J AND AARTS MGM. Unpublished thesis chapter.
- WEIGEL, D, AND MOTT, R. 2009. The 1001 genomes project for *Arabidopsis thaliana*. *Genome biology* 10: 107.
- WUNDER T, LIU Q, ASEVA E, BONARDI V, LEISTER D AND PRIBIL M. 2013. Control of STN7 transcript abundance and transient STN7 dimerisation are involved in the regulation of STN7 activity. *Planta* 237: 541-558.
- WONG H-K, CHAN H-K, CORUZZI GM AND LAM H-M. 2004. Correlation of ASN2 gene expression with ammonium metabolism in *Arabidopsis*. *Plant physiology* 134: 332-338.
- ZHANG Y, WERLING U AND EDELMANN W. 2012. SLiCE: a novel bacterial cell extract-based DNA cloning method. *Nucleic acids research* 40: e55.

Supplemental data

Tables

Table S1: Primer information

Purpose	Name	Sequence	Amplicon length	Tm	Remark
Molecular cloning	ASN2_F_attB1	GGGGACAAGTTTGTACAAAAAAGCAGGCTCTATCAAAGAGAATACCCAATGGTCTC		63	primer set 1
	ASN2_R_attB2	GGGGACCACTTTGTACAAGAAAGCTGGGTCTGATGAAGAGCGACTCCGCT		63	
	PAH2_F_attB1	GGGGACAAGTTTGTACAAAAAAGCAGGCTCTCACCTCGGAGTCGGTCTT		63	primer set 1
	PAH2_R_attB2	GGGGACCACTTTGTACAAGAAAGCTGGTCTGAATCTTTATCATCGCCCA		63	
	ASN2_GATEWAY_F	GGGGACAAGTTTGTACAAAAAAGCAGGCTCTCAAAGCAACAATGGAATTGG		?	primer set 2
	ASN2_GATEWAY_R	GGGGACCACTTTGTACAAGAAAGCTGGTCTCACAAGCCAGAACATGCACAA		?	
	PAH2_GATEWAY_F	GGGGACAAGTTTGTACAAAAAAGCAGGCTCTCGGTGTTGAGTGAATGATG		X	primer set 2
	PAH2_GATEWAY_R	GGGGACCACTTTGTACAAGAAAGCTGGTCTCATCACCAGCTTCCCAATG		X	
	PAH2_gibson_1.F	TCCTTATGTACAAGTAAAGCGTCACTCGGAGTCGGTCTTCG		64	
	PAH2_gibson_1.R	CGCTTATGTACTACTGATGATGATGATAAAGATGATGATTTGTCTT		64	
	PAH2_gibson_2.F	IATCATCAGTATCACATAAGCGATGGAGGAGGC		64	
	PAH2_gibson_2.R	CGATCGAAAAATGAATGCCGTCGGTAGGAT		64	
	PAH2_gibson_3.F	GGCATTCATTTTTCGATCGGAAAAGTCAACGAAAGT		66	
	PAH2_gibson_3.R	CTGCAGGCGCCGCACTGAATCTTATCATCGCCCAACATTGT		66	
	sequencing ASN2_F1	CGACGTCGATGCTCCCG	1152 bp	60	
	sequencing ASN2_R1	CAGTGACAGCGAGCTTGTCT		60	
	sequencing ASN2_F2	IGATTGAGGCACAGAGTCTGAT	997 bp	60	
	sequencing ASN2_R2	ACGGAGGATTGTACCACCTCC		60	
	sequencing ASN2_F3	CGGAGATGAAAGCCTTAGTGAT	985 bp	60	
	sequencing ASN2_R3	ICCCAGTATTTTCATCAGAACCTTCCCC		60	
sequencing ASN2_F4	CAGGACGGGATAGACGCGA	1001 bp	60		
sequencing ASN2_R4	GCAGCACTCTGCTCAGGAAAT		60		
sequencing ASN2_F5	IGTCTCTGATACTATGCTGTCAAACGCAA	965 bp	60		
sequencing ASN2_R5	GGCGGGAACGACAATCTGAT		60		
Triple x	ASN2_seqR_half	CCCAGTATTTTCATCAGAACC	~2000 bp	54	ASN2 gene product
	SALK_146656QF	TTGCATCGACAACTCTCAAG		54	
	ASN2_seqR_half	CCCAGTATTTTCATCAGAACC	~1500 bp	54	ASN2 T-DNA product
	LB1.3	ATTTTGCCGATTTTCGGAAC		54	
	SALK_042970_LP	TAATTTTGGCTTGTGTTGGG	1070 bp	54	PAH1 gene product
	SALK_042970_RP	GTITTTGGTCAGCTCTGACTGC		54	
	SALK_042970_RP	GTITTTGGTCAGCTCTGACTGC	~600 bp	54	PAH1 T-DNA product
	LB1.3	ATTTTGCCGATTTTCGGAAC		54	
	SALK_047457_LP	AATGCAACAGGTAGACGCAAG	1105 bp	54	PAH2 gene product
	SALK_047457_RP	GCAAAATGCAACAACAGTTG		54	
SALK_047457_RP	GCAAAATGCAACAACAGTTG	~600 bp	54	PAH2 T-DNA product	
LB1.3	ATTTTGCCGATTTTCGGAAC		54		
qRT-PCR	UBQ7_1F	GCAGCGACACCATCGACAAT		59,35	
	UBQ7_1R	AGGTCCGGCCATCTCCAAT		59,35	
	CB5-E_3F	TTGCAAGTGTGCTGTGACCA		59,35	
	CB5-E_3R	TGATCATCTCGGAGCGGATG		59,35	
	Q_DGD1_F2	TTCTTCTCCTCCTCCATT		57,3	
	Q_DGD1_R2	IATCTCTTTGGGAAGCAGCA		57,3	
	Q_DGD2_F1	CCTGGAGCTTCTGCTTCT		59,35	
	Q_DGD2_R1	GCTGCGACTCAAGAATACCC		59,35	
	Q_MGD1_F1	IGTTTTGGGTGAGGAGGGATT		57,3	
	Q_MGD1_R1	CAGAAGCTCTGTGACCACCA		57,3	
	Q_MGD2_F1	CCGTCAACCCATCATACA		57,3	
	Q_MGD2_R1	ICCGATCTGGATAAGCTCAA		57,3	
	Q_MGD3_F1	ATTAATGGGAGGGGGTGAAG		55	
	Q_MGD3_R1	GGCCGCATATGACAATCAA		55	
	SALK_146656QF	TTGCATCGACAACTCTCAAG		55,5	qRT-PCR of ASN2
	at5g65010_QR1	CTCCAATCAGGACCTCTG		55,5	
	PAH1_QF	CCTGTTGCCATCTCCCTT		59,3	qRT-PCR of PAH1
	PAH1_QR	ITACAACCCGTTCTATGCCGG		59,3	primer set 1
	PAH1_QF2	TCAGCTCTGACTGTCCAGA		60	
	PAH1_QR2	TGGATTCCCATCTCTGTGAT		60	primer set 2
	at5g42870_QF	ICTTCCATTACAGTACGAG		57,3	qRT-PCR of PAH2
	at5g42870_QR	GGTGATGAAGCTGAGACTAC		57,3	primer set 1
	PAH2_QF2	CCATTCTTCAAACCCCTTG		59,6	
	PAH2_QR2	IAGGTCCGTTTCATCCATTG		59,6	primer set 2

Table S2: Tukey test on fresh weight on plants grown at 100 $\mu\text{mol photons m}^{-2} \text{s}^{-1}$

Sample	N	Subset
		1
asn2-1pah1	7	,06471
pah1pah2	6	,06783
asn2-1	4	,07900
asn2-1pah2	3	,08767
pah2	6	,10283
pah1	7	,12086
col-0	7	,12414
Sig.		,286

Table S3: Tukey test on fresh weight on plants grown at 200 $\mu\text{mol photons m}^{-2} \text{s}^{-1}$

Sample	N	Subset			
		1	2	3	4
triple	9	,19967			
asn2-1	7	,20057			
asn2-1pah2	2	,21350	,21350		
asn2-1pah1	9	,29511	,29511		
pah2	9	,33589	,33589		
pah1pah2	9	,33733	,33733		
pah1	9	,44656	,44656	,44656	
ga-0	9		,51067	,51067	,51067
col-0	9			,68311	,68311
ts-1	9				,76322
Sig.		,215	,061	,267	,190

Table S4: Tukey test on fresh weight on plants grown at 400 $\mu\text{mol photons m}^{-2} \text{s}^{-1}$

Sample	N	Subset			
		1	2	3	4
asn2-1pah1	9	,48222			
triple	8	,48463	,48463		
ga-0	8	,93713	,93713	,93713	
asn2-1pah2	5	,99880	,99880	,99880	,99880
pah1pah2	9	1,04122	1,04122	1,04122	1,04122
ts-1	8		1,12663	1,12663	1,12663
pah1	9			1,37889	1,37889
asn2-1	8			1,38163	1,38163
pah2	7			1,38200	1,38200
col-0	9				1,58300
Sig.		,145	,052	,430	,108

Table S5: Tukey test on fresh weight on plants grown at 550 $\mu\text{mol photons m}^{-2} \text{s}^{-1}$

Sample	N	Subset		
		1	2	3
asn2-1pah1	5	1,24820		
triple	6	1,41483	1,41483	
pah2	6	1,72083	1,72083	1,72083
pah1pah2	6	1,81533	1,81533	1,81533
ga-0	6	1,89417	1,89417	1,89417
asn2-1	6	1,93633	1,93633	1,93633
pah1	6	2,32317	2,32317	2,32317
ts-1	5		2,51020	2,51020
col-0	5			2,90440
Sig.		,144	,129	,077

Protocols

Preparation of electro competent DB3.1 *E.coli* cells

Materials:

~ 2L sterile cold water (0 °C) and 0,5 ml DMSO, ~ 60 sterile tubes

Plate with fresh DB3.1 colonies

Cooled centrifuge (Ask for centrifuge on first floor), Buckets (Beckmann tubes, 250 ml), dry ice, or alternatively liquid nitrogen.

2x 2L erlenmeyer with 500 ml LB, 1x 100 ml Erlenmeyer with 75 ml LB.

Protocol:

1. Make a full grown o/n culture at 37°C, 300 rpm, in LB broth (75 ml) starting from one or a few single colonies of the DB3.1 strain. Pre-cool o/n ~2 L of sterile water in Fridge.
2. Inoculate 2x 500 ml LB broth in 2L flasks with ~15 ml o/n culture to OD₆₀₀ of max 0,2.
3. Grow at 16 °C, 250 rpm, till OD₆₀₀ ≈ 0,4 (takes about 4-8 hrs). Meanwhile pre-cool centrifuge, eppendorf tubes, centrifuge buckets, tubes, etc..

Note: If growing at 16 °C takes too long, increase temperature

4. Transfer cultures to 4x Beckmann tubes and spin 20 min, 5000 rpm at 4 °C.
5. Resuspend pellets in 4x 175 ml 0 °C cold water. Dissolve by gently pipetting and decanting (preferably do not vortex).
6. Spin 20 min 5000 rpm (max) at 4 °C.
7. Resuspend in 4x 50 ml 0 °C cold water. Dissolve by gently pipetting and decanting.
8. Spin 20 min 5000 rpm (max) at 4 °C.
9. Resuspend in 2x 8 ml 0 °C cold water and transfer culture to falcon tube.
10. Spin 10 min 5000 rpm (max) at 4 °C.

11. Resuspend the pellets in a 7% DMSO solution: 225 μ l DMSO + 3 ml 0 $^{\circ}$ C cold water.
12. Snap freeze (preferably on dry ice) 50 μ l aliquots into pre-cooled (- 80 $^{\circ}$ C) Eppendorf tubes (use combitip) and store tubes in -80 $^{\circ}$ C freezer.

Preparation of electro-competent cells

- Inoculate the appropriate E.coli strain (Used: DH5 α F'), preferentially from a fresh plate or from a frozen stock, in 5 ml LB medium and incubate overnight at 37 $^{\circ}$ C.
- Dilute 1:100 by adding the preculture to 500 ml medium without NaCl. Grow with vigorous shaking at 37 $^{\circ}$ C until the OD600 is 0,5 – 0,8 (~3-4 hours).
- Spin 10 min. at 4000 rpm at 4 $^{\circ}$ C.
- Resuspend the bacterial pellet in 500 ml ice-cold mQ.
- Spin 10 min. at 4000 rpm and 4 $^{\circ}$ C.
- Resuspend the pellet in 500 ml ice-cold mQ.
- Spin 10 min. at 4000 rpm and 4 $^{\circ}$ C
- Resuspend in 40 ml 8,7% ice-cold Glycerol.
- Spin 10 min. at 4000 rpm and 4 $^{\circ}$ C.
- Resuspend the pellet in 1.5 ml of 8,7% ice-cold Glycerol.
- Aliquot in ~80 μ l fractions in precooled Eppendorf tubes.
- Store at -80 $^{\circ}$ C.

Preparation before:

Autoclave all:

500 ml LB medium (without NaCl!!!) in a 2 Liter erlenmeyer.

3 large PVC buckets

2 small PVC tubes

1 liter mQ

8,7% glycerol (200 ml)

Eppendorf tubes.

Transformation by electroporation

1. Prepare 2 LB/AXI plates for each ligation-reaction, be sure the plates are not too wet. Dry the plates 15 min in Flow cabinet.
2. Cool the electroporation cuvettes on ice, or put them at -20 $^{\circ}$ C 30 minutes before use.
3. Turn on the Micro pulser. Adjust the pulse to the size of the cuvette: for 0,1 cm cuvette (Braun cap) use 1.8 kV, for 0,2 cm cuvette (green cap) use 2.5 kV.
4. Centrifuge the ligation reaction to collect the contents at the bottom.
5. Remove the frozen competent cells from -80 $^{\circ}$ C and place them on ice, it will take about 5 minutes till thaw.
6. Add 2 μ l ligation mixture to the competent cells on ice, gently flick the tube to mix and put it back on ice.

7. Transfer all into the gap of the electroporation cuvette, try not to introduce air bubbles. Flick against the cuvette till the cells are equally spread in the cuvette.
8. Put the cuvette between the metal clamps in the micro pulser and give a pulse.
9. Quickly add 1 ml SOC medium (preheated to 37°C) to the cuvette and pipette up and down smoothly to suspend the cells.
10. Let the fragile cells recover for 1 hour at 37°C with gentle shaking (150 rpm).
11. Dilute the cells 10, 10⁻¹, 10⁻² or more in LB and plate out 100 ul of each transformation. The dilution depends on the success of transformation.
12. Incubate the plates overnight at 37°C

Solutions needed:

LB-medium (1 L):

- Dissolve 10 g tryptone, 5 g yeast extract, and 10 g NaCl in 950 mL deionized water.
- Adjust the pH of the medium to 7.0 using 1N NaOH and bring volume up to 1 liter.
- Autoclave on liquid cycle for 20 min at 15 psi. Allow solution to cool to 55°C, and add antibiotic if needed 4. Store at room temperature or +4°C.

LB agar-plates:

- Prepare LB medium as above, but add 15 g/L agar before autoclaving.
- After autoclaving, cool to approx. 55°C, add antibiotic (if needed), and pour into petridishes.
- Let harden, then invert and store at +4°C in the dark.

SOC-medium:

2.0 g Bacto-Tryptone

0.5 g Yeast-Extract

1 ml 1 M NaCl

0.25 ml 1 M KCl

2 ml 1 M Mg⁺⁺stock (sterilize by autoclaving)

2 ml 1 M Glucose (filter sterilized)

Add Tryptone, Yeast, NaCl and KCl to 97 ml water, autoclave and cool to Room Temperature. Make 2 ml aliquots and store at -20°C.

CTAB DNA isolation

1. Make sure you start with ground plant material, either ground by hand or by the shaker
2. Centrifuge samples briefly to bring down tissue dust.
3. Add 300 uL CTAB, close the tubes and heat in a 65 C waterbath for 30 mins
4. Cool to room temperature

5. Add 300 μ L chloroform (IN FUMEHOOD) Close the tubes and mix vigorously for 10-20 seconds.
6. Centrifuge at 3250 rpm for 15 mins. If the centrifuge doesn't have this step, you can do 3300 rpm as well.
7. During centrifugation, prepare tubes with 200 μ L of ice cold isopropanol/isopropyl alcohol (- 20 c). Keep on ice!
8. Transfer 200 μ L of the chloroform extracted supernatant to the new tubes. Be very careful not to pipet any of the goo in the middle layer.
9. Mix gently
10. Centrifuge at 3250 rpm for 15 mins.
11. Gently pour off the liquid in a waste beaker. Be careful not to tip out the pellet!
12. Was pellet with 200 μ L of 70 % ethanol
13. Flick the tubes gently to wash and centrifuge 3250 rpm for 15 mins.
14. Pour off the liquid
15. Repeat step 12
16. Pour off the liquid carefully and make sure you get rid of as much ethanol as possible by keeping tubes upside down on paper towels or careful pipetting
17. Air dry the tubes for about 30 mins. You can speed this process up by putting it in a stove for 10 mins at 65 C but be careful not to overheat it
18. Resuspend pellet in 50 μ L of TE buffer or (autoclaved) MQ water.

1 L 2x CTAB:

20 g CTAB

81.82 gr NaCl

100 ml 1M Tris, pH 8

40 mL 0.5 M EDTA

CTAB goes into solution slowly, and can release toxic fumes when heated so do this in a FUMEHOOD

Final cc: 2 % CTAB, 1.4M NaCl, 100 mM Tris, 20mM EDTA.

RNA isolation

Sample preparation and general considerations

Freeze and grind samples in liquid nitrogen with the help of a microfuge pestle coupled to a drill (Protocol 1) or with mortar and pestle (Protocol 2). All centrifugations are at maximum speed in a table top microfuge at room temperature unless otherwise indicated. In both protocols, optionally after step 4: Use a 0.2 μ l aliquot as a template for PCR to check for genomic DNA contamination (a 500bp amplicon from a β -tubulin gene is normally used). If necessary, more DNase can be added to contaminated samples and incubated for another 15 min at 37°C before continuing the protocols.

- Protocol 1 - (vegetative tissues)

1. Add 300 μ l of cell lysis solution (2% SDS, 68 mM sodium citrate, 132 mM citric acid, 1 mM EDTA) to ground tissue and homogenize quickly by vortexing 2 s and inverting and flicking the tube gently. Leave tubes at room temperature up to 5 min.
2. Add 100 μ l of protein-DNA precipitation solution (4 M NaCl , 16 mM sodium citrate, 32 mM citric acid) to the cell lysate, mix inverting the tubes gently and incubate at 4°C for at least 10 min. Spin at 4°C for 10 min.
3. Transfer s/n to a new SMT, add 300 μ l isopropanol and mix the sample by inverting gently the tube. Spin 4 min and carefully pour off the s/n. Wash pellet with 70% ethanol, air-dry RNA and resuspend in 25 μ l DEPC- water.
4. Add 3 μ l 10X DNase buffer and 2 μ l (2 units) of DNase I (RQ1 RNase-free DNase; Promega M6101). Incubate 30 min at 37°C.
5. Add 70 μ l DEPC-water to the 30 μ l of RNA, 50 μ l of NH₄Ac 7.5 M (sodium acetate can also be used) and 400 μ l 100% ethanol and mix well. Spin 20 min at 4°C, wash pellet with 70% ethanol, air-dry RNA and resuspend in 20 μ l DEPC-water.

cDNA synthesis

Before starting the cDNA synthesis, the RNA concentrations of all samples should be normalized to be the same.

Reaction Set Up

Component	Volume per reaction
5x iScript Reaction Mix	4 μ l
iScript Reverse Transcriptase	1 μ l
Nuclease-free water	x μ l
RNA template (100fg to 1 μ g Total RNA)*	x μ l
<hr/>	
Total Volume	20 μ l

Reaction Protocol

Incubate complete reaction mix:
5 minutes at 25°C
30 minutes at 42°C
5 minutes at 85°C
Hold at 4°C (optional)

The cDNA should always be diluted 10X before you can use it in qPCR. This is because reagents from the cDNA synthesis interfere in the qPCR reaction. If you dilute 10X this interference can be neglected.

qRT-PCR

Reaction Set Up

SYBR Green Supermix	5 μ L
Primer 1 (3 μ M)	0.5 μ L
Primer 2 (3 μ M)	0.5 μ L
Sterile water	1 μ L
cDNA template	3 μ L
	10 μL

Reaction Protocol

1. 3 minutes 95°C
2. 10 seconds 95°C
3. 15 seconds ... °C (Tm)
4. 23 seconds 72°C + plate read
5. Go to step 2 for 39 times
6. Melt curve 55°C-95°C for 5 seconds + plate read